ISSN 1454-8518

ANNALS OF THE UNIVERSITY OF PETROŞANI

ELECTRICAL ENGINEERING

VOL. 17 (XLIV)

UNIVERSITAS PUBLISHING HOUSE
PETROŞANI - ROMANIA 2015

ISSN 1454-8518

Editorial office address: Ec. Radu Ioan, University of Petroşani, 20 University Street, 332006 Petroşani, Romania, Phone: (40) 254/54.29.94; 54.25.80; 54.25.81; 54.33.82; Fax: (40) 254/54.34.91; 54.62.38,
Contact person: **Susana ARAD**, e-mail: susanaarad@yahoo.com
This publication is with international distribution. It is sending in 28th countries.

CONTENTS

Annals of the University of Petrosani, Electrical Engineering, 17 (2015)

USING NI-USB DATA AQUISITION SYSTEMS TO STUDY THE CONNECTING OF INDUCTIVE LOADS, IN MATLAB MEDIUM

TITU NICULESCU[1], FLORIN GABRIEL POPESCU[2], MARIUS DANIEL MARCU[3], RĂZVAN SLUSARIUC[4]

Abstract: The paper presents a new and modern method to study the transient phenomena that occurs when connecting the reactive charges to an AC power source, using the MATLAB-SIMULINK software package. It is known that NI-USB data acquisition systems manufactured by National Instruments are not recognized by the Simulink software package in 64-bit systems. That is why a 32-bit system is obligatory. From this point of view, the article presents a method by which this disadvantage is eliminated, making the data acquisition process possible in Simulink software package.

Keywords: Capacitive circuit, Data acquisition, Diagrams, Electrical diagram, MATLAB - Simulink, NI-USB

1. INTRODUCTION

Data acquisition systems of the NI-USB type, manufactured by National Instruments, allow real-time evaluation of analog measurements in various practical situations. These quantities can be read by the MATLAB software, but cannot be processed in Simulink because MathWorks Incorporated does not offer support for this software in 64-bit systems [7]. The paper presents a method that makes this possible and studies the case when an inductive-capacitive load is connected to a voltage power source, with a data acquisition system in Simulink on 64-bit systems [9].

[1] *Associate Professor, Eng., PhD, University of Petrosani, Romania*
[2] *Lecturer, Eng, PhD, University of Petrosani, Romania*
[3] *Associate Professor, Eng., PhD, University of Petrosani, Romania*
[4] *Assistant, , Eng, PhD, University of Petrosani, Romania*

2. INTERFACE CIRCUITS NECESSARY FOR STUDY THE PHENOMENA

For the experimental evaluation of these parameters, a data acquisition system manufactured by National Instruments was used, namely the NI USB-6003 type. The graphics and the electrical diagram presented in Fig.2 was created using the MATLAB 2014b software. The inductive circuit is connected to the AC voltage through a capacitor C and the DAQ input voltage levels are obtained using resistive dividers. A differential measurement was chosen to perform calculations [6].

To eliminate the risk of connecting directly the AC phase voltage to the input of the data acquisition system, symmetrical voltage dividers were used and the analog inputs of the measuring system are connected in parallel with the median divider resistors Ri0 and Ri1. To protect the analog inputs of data acquisition system to any voltage surge, the DZ Zener diodes were used (Fig.1).

The measuring mode is a differential one, because it allows accurate measurements for low voltage amplitudes (below 1V).

The used system for data acquisition has the following important parameters:

- 8 analog inputs (16-bit resolution, 100 kS/s);
- 2 analog outputs (16-bit, 5 kS/s/ch); 13 digital I/O lines; one 32-bit counter;
- Lightweight and BUS powered for easy portability;
- Easy to install sensors and signals with screw-terminal connectivity.

The system is compatible with MATLAB software, but not with the Simulink package, because the Data Acquisition Toolbox package does not appear in its graphical interface on 64-bit operating systems.

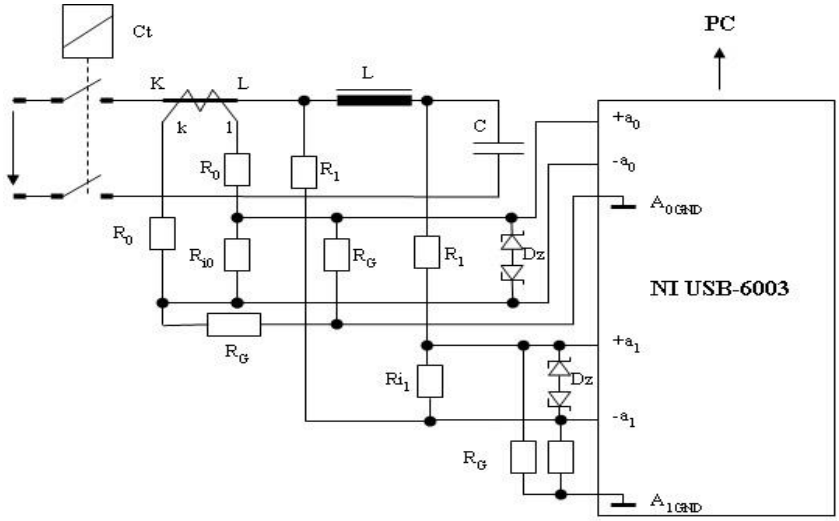

Fig. 1 Electrical diagram of measurement system for inductive loads

To study switching transient inductive-capacitive loads, it was considered the connecting an inductive capacitive load to an alternating power supply, made with the following values of electrical parameters:

U=220V; R=1,2Ω; L=2 mH; C=100μF.

In this case the diagram from Fig.2 is obtained.

Data acquisition is made with the Ni-USB 6003 system which has a sampling frequency of 100ks/sec. The sequence of MATLAB program that reads current and voltage inputs and make data acquisition is shown as it follows:

```
s = daq.createSession('ni');
addAnalogInputChannel(s,'Dev1', 0, 'Voltage');
addAnalogInputChannel(s,'Dev1', 1, 'Voltage');
s.Rate = 45000;
s.DurationInSeconds = 1.5;
[data,time] = s.startForeground;
figure;
data(:,1)=data(:,1)*163;
data(:,2)=data(:,2)*27;
[ax,p1,p2] = plotyy(time,data(:,1),time,data(:,2),'plot');
ylabel(ax(1),'Voltage[V]');  % label left y-axis
ylabel(ax(2),'Current[A]');  % label right y-axis
xlabel('Time[secs]');    % label x-axis
grid;
```

where *163* and *27* are values dependent on resistors values of interface from Fig.3. These values are dependent on the input resistive dividers values of the measurement system (163 is the value of $2R_1/R_{i1}$ and 27 represent the value of $2R_0/R_{i0}$).

To run this code, it needs a system NI USB-6000 series connected to the PC and installing the driver from the National Instruments website. The first part of this code represent data acquisition with a rate of the 45 kS/sec, and the acquisition time is 1,5 sec. The second part of the code represent the ploting mode of voltage and current. Because the acquisition time is relatively high (1.5 sec), after completion of the acquisition process, one can decrease this time to 0.1 sec by focusing on the event (click **Edit figure**>**Axes properties**…>**xLimits**).

The sampling frequency is divided by two because there are two inputs to read. Therefore it was used a sampling rate of 45 kS/sec for each channel.

Connecting regime from Fig.2 primarily highlights an oscillating process for current and coil voltage. In the first moment of connection an overcurrent appears, with a peak of over 30A. The overvoltage peak is almost 400V in the first moment, after which these values are stabilized to the oscillating values.

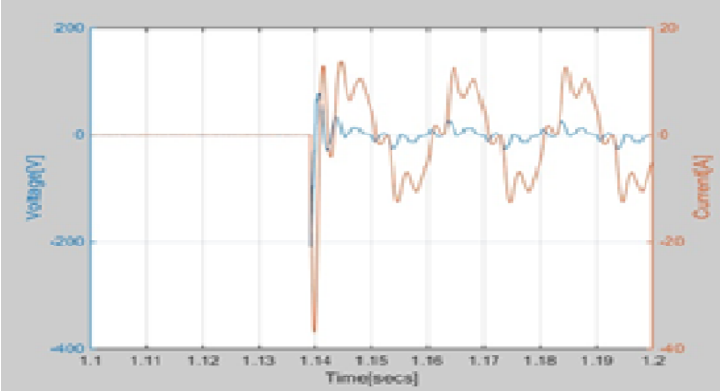

Fig. 2 Connecting an inductive capacitive load

3. MEASUREMENT PROCESSING IN SIMULINK SOFTWARE PACKAGE

Experimental measurements were made with a data acquisition system type NI USB-6003 with a rate of 100kS/ sec., and the measurements were processed by 2014b MATLAB version, which recognizes only data acquisition system in MATLAB, not in Simulink. Data processing in Simulink involves the following steps:

- It makes the appropriate data acquisition in MATLAB (using specific program lines for data acquisition system type);
- It saves the ***Workspace*** generated by the measurement (for further processing);
- The ***Data*** file from the ***Workspace*** opens;
- The ***Time*** file from the ***Workspace*** opens;
- Undock command is given to these files (Fig.4);
- The ***Time*** column is copied in the ***Data*** file and it's placed at the beginning of the columns (Fig.5).
- It executes the **Dock *Variables*** command and saves the new ***Workspace***.

At this moment the ***Data*** folder from the ***Workspace*** can be read from a Simulink simulation model. This is shown in Fig.3:

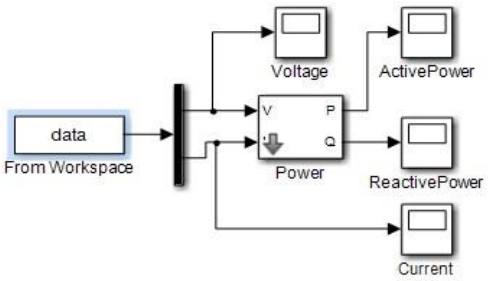

Fig. 3 Simulink model for reactive load connecting

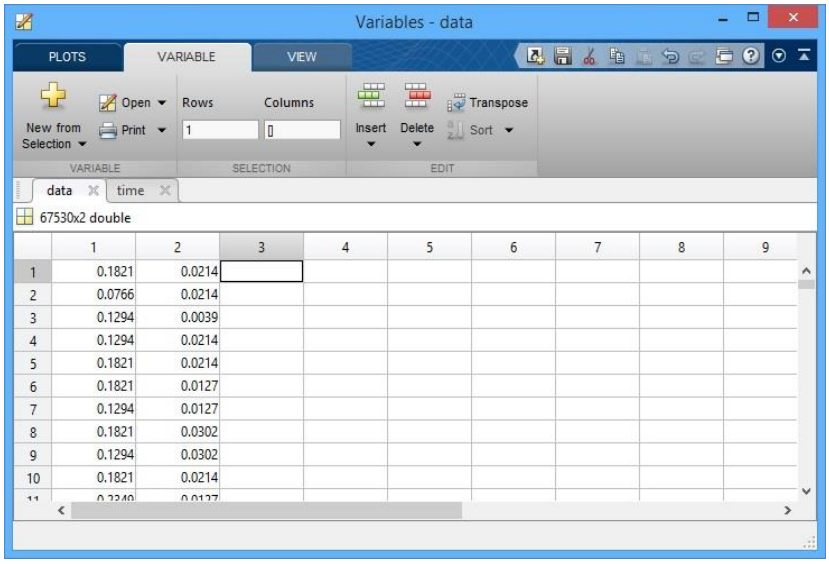

	1	2	3	4	5	6	7	8	9
1	0.1821	0.0214							
2	0.0766	0.0214							
3	0.1294	0.0039							
4	0.1294	0.0214							
5	0.1821	0.0214							
6	0.1821	0.0127							
7	0.1294	0.0127							
8	0.1821	0.0302							
9	0.1294	0.0302							
10	0.1821	0.0214							

Fig. 4 Original content of the *Data* folder from the *Workspace*

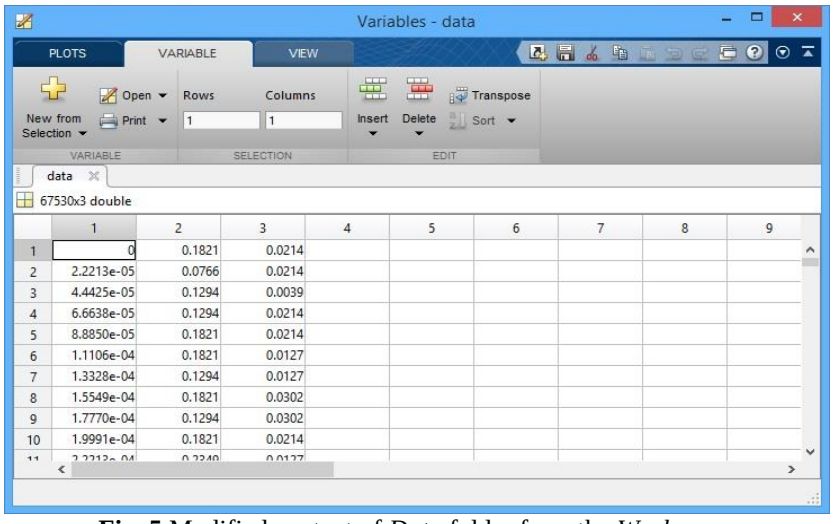

	1	2	3	4	5	6	7	8	9
1	0	0.1821	0.0214						
2	2.2213e-05	0.0766	0.0214						
3	4.4425e-05	0.1294	0.0039						
4	6.6638e-05	0.1294	0.0214						
5	8.8850e-05	0.1821	0.0214						
6	1.1106e-04	0.1821	0.0127						
7	1.3328e-04	0.1294	0.0127						
8	1.5549e-04	0.1821	0.0302						
9	1.7770e-04	0.1294	0.0302						
10	1.9991e-04	0.1821	0.0214						

Fig. 5 Modified content of *Data* folder from the *Workspace*

The first representative case for connecting the capacitive inductive load, leads to the following charts for the inductor voltage, circuit current, and the powers dissipated in the coil.

As one can observe, the coil voltage and current diagrams (Fig.6 and Fig.7) show the identical dependences with Fig.2 where the forms were obtained by data acquisition directly in MATLAB, by programing. The MATLAB program is presented in the paragraph 2.

Fig. 6 Voltage variation on coil when connection is initiated

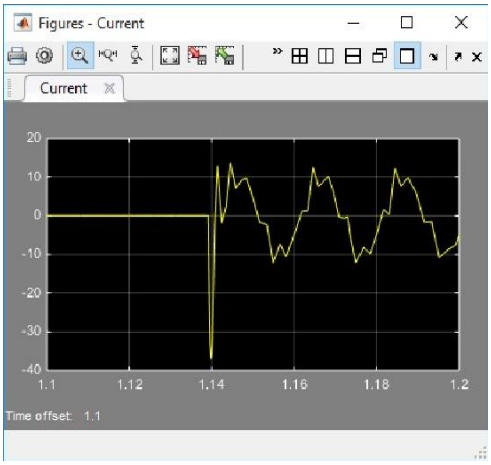

Fig. 7 Current variation on coil at connecting

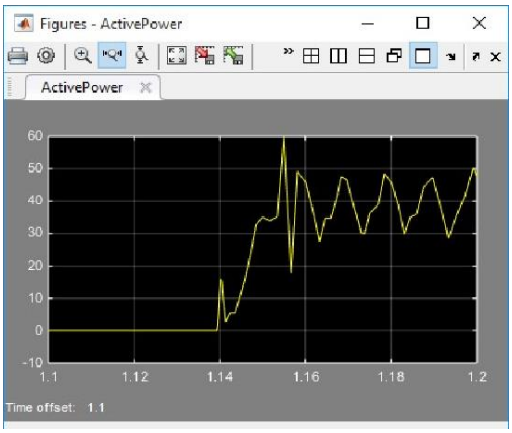

Fig. 8 Active power variation on coil resistance at connecting

Fig. 9 Reactive power variation on coil at connecting

Fig. 8 and Fig. 9 represent diagrams of the active and reactive power variation during the commutation process. An inductive load of 2 mH was connected to an alternating power source.

Because of the capacitor, the oscillating process occurs in both the current curve and the coil voltage. The value of capacitance that made the connection process was of 100 μF. The voltage oscillations and current circuit right after the connection was initiated, are accompanied by oscillations of active and reactive power. Measurement was done in the time interval of 1.1-1.2 sec.

4. CONCLUSIONS

This analysis method allows the study of transient electrical phenomena on 64-bit operating systems. In this case, in Simulink does not appear the Data Acquisition Toolbox package, which is specific to the 32-bit operating systems.

We have to mention that the transient regime for connecting the reactive loads to an AC power source depends on moment of connecting, given by Ψ angle (initial phase) from analytic expressions of voltage and current. In this paper we considered a representative case of several measurements that emphasize the higher values of voltage and current occurring immediately after connecting.

REFERENCES

[1] **Hortopan Ghe**. *Aparate Electrice*. 1980th E.D.P. Bucharest, 1980.

[2] **Marin Ghinea, Virgiliu Firteanu**, *MATLAB, Calcul numeric-grafică-aplicații*. 2000 ed. Ed. Teora; 2000.

[3] **Marcu M.D., Popescu F.G., Niculescu T., Pana L., Handra A.D.,** *Simulation of power active filter using instantaneous reactive power theory*. Harmonics and Quality of Power (ICHQP), IEEE 16th International Conference, Page(s):581 – 585, Bucharest, Romania, 25-28 May, 2014.

[4] **Nicolae Golovanov** s.a.. *Consumatori de energie electrica. Materiale, Masurari, Aparate, Instalatii*. ED. AGIR, Bucharest 2009.

[5] **Niculescu Titu**. *Analiza circuitelor electrice prin simulare in spatiul MATLAB*. 2006th ed. Petrosani: 2006.

[6] **Niculescu Titu**. *Study of Inductive-Capacitice Series Circuits Using the Simulink Software Package*. In: inTech, editor. Technology and Engineering Applications of Simulink. 2012th ed. 2012, Chapter 2.

[7] **Niculescu Titu**. *Study of transient phenomena using NI-USB data aquisition systems in Matlab-Simulink medium on 64bit operating systems*. Journal of Advanced Computer Sciense&Technology. 2015; ID: 4518.

[8] **Niculescu Titu**. *Transitory phenomena in capacitive circuits connected to an AC source*. In: Proceedings of the 4th International Conference on Circuits, Systems, Control, Signals - CSCS'13; 2013; Valencia, Spania:pp. 162-166.

[9] **Niculescu Titu, Marcu Marius, Popescu Florin Gabriel**. *Study of transitory phenomena at connecting the capacitive loads to an AC power source*. Journal of Advanced Computer Sciense&Technology. 2015: D: 4518.

[10] **Simona Halunga-Fratu, Octavian Fratu**. *Simularea sistemelor de transmisie analogice si digitale folosind mediul MATLAB/SIMULINK*. 2004th Bucharest: ED. MatrixRom; 2004.

[11] **Uțu I., Samoilă L.,** *Senzori şi instrumentaţie pentru sisteme electromecanice,* Editura Universitas, ISBN 978-973-741-208-9, pp. 222, Petroşani, 2010.

CONFORMITY ASSESSMENT OF CONVEYOR BELTS AND BELT CONVEYORS WITH THE ESSENTIAL SAFETY AND HEALTH REQUIREMENTS OF EUROPEAN DIRECTIVE ATEX 94/9/EC

FLORIN ADRIAN PĂUN[1], MIHAELA PĂRĂIAN[2], NICULINA VĂTAVU[3], ADRIAN JURCA[4]

Abstract: Belt conveyors have been used for a long time in most of the industrial branches, as well as in places where the likelihood of explosive atmospheres occurrence exists. Therefore, the use of conveyor belts in hazardous environments requires fulfilling certain requirements, very important for the safety level to be provided, to prevent ignition sources. This paper highlights the main aspects related to assessment of explosion risk when using conveyor belts and certification of belt conformity with the applicable essential health and safety requirements performed by a third party body.

Keywords: potentially explosive atmospheres, explosion risk, conveyor belt, conveyer, risk assessment.

1. INTRODUCTION

Conveyor belts are widely used within various industrial activities, as components of transportation installations and systems for solid materials.

The field of use of conveyor belts is a wide one, as these can be employed both in underground and surface conveying installations of many applications [4].

At the same time, conveyor belts can be used in environments where potentially explosive atmospheres are present or likely to occur generated either by the conveyed material or other external sources.

Generally, in industrial areas where combustible/ flammable substances are processed during normal operation, due to technological processes or processed during

[1] *Ph. D.Eng., scientific researcher III, INDC-INSEMEX Petroşani*
[2] *Ph. D.Eng., scientific researcher I, INDC-INSEMEX Petroşani*
[3] *Ph. D.Eng., scientific researcher III, INDC-INSEMEX Petroşani*
[4] *Ph. D.Eng., scientific researcher III, INDC-INSEMEX Petroşani*

normal operation, due to technological processes or accidental leakages or releases, explosive mixtures of gas, vapors, mists or powders and air are likely to occur. To mitigate explosion risks in these industrial environments with potentially explosive atmospheres, broadly named "Ex Zones", the equipment employed shall be of a special construction for explosive atmosphere that shall not generate energy sources that could initiate an explosion [1], [3].

Thus results that the conveyor belts used in various transportation installations have to fulfill the essential safety requirements regarding explosion dangers that aims on one side to prevent formation of an explosive atmosphere around the installation and on the other side prevention (avoidance) of sources of ignition of the explosive atmosphere, as for example the ignition sources of electrostatic nature or due to hot surfaces and incandescent particles which might occur due to friction [5].

The essential safety and health requirements are transposed in a series of European standards with provisions related to construction, testing and marking of conveyor belts for potentially explosive atmospheres.

Conveyor belts testing for certification is of a particular importance having in view the existing explosion risk that has to be minimized in order to ensure life safety and human health and in order to prevent goods and environment damage, as well as for a free circulation of products when they fulfill the essential safety requirements, at European level.

2. IGNITION RISK ASSESSMENT RELATED TO FULFILLING THE ESSENTIAL SAFETY AND HEALTH REQUIREMENTS IN THE ATEX DIRECTIVE FOR CONVEYOR BELTS AND BELT CONVEYORS

Assessment of the ignition risk when using equipment, protective systems and components in environments with flammable substances that could generate fires and explosions has a special importance when aiming to ensure workers safety and health. According to the legislation in force, responsibility for risk assessment and adopting the adequate protective measures to ensure an acceptable safety level, belongs both to equipment manufacturers aiming to place on the market products with a certain level of protection, and to employers which have to select equipment adequate to the risk of explosive atmospheres occurrence in the areas where these are placed for operation.

The protection concepts have in view firstly making use of some equipment that can ensure protection by preventing intrinsic ignition sources, and added to this if necessary, additional protective devices and maintenance / use measures, specific to the foreseeable field of use [8], [11].

Concerning this, not only conveyor belts but also belt conveyors operating in environments with potentially explosive atmosphere and all their components have to be submitted to an official risk analysis, well documented, that aims to identify and list all potential ignition sources in the equipment, and the measures to be applied to prevent them from becoming efficient. Examples of such sources include: hot surfaces, open flames, hot liquids / gases, mechanically generated sparks, alumino-thermal

reactions, auto-ignition of dusts, electric arcs and static electricity discharges [8], [9].For explosion prevention and protection there are protective measures that have to be applied both in order to prevent explosive atmospheres and to avoid ignition sources.

The explosion protection principle can be expressed as: the likelihood that an ignition source occurs at the same time with an explosive atmosphere should be reduced to a minimum. As case might be, measures for explosion mitigation could be required. Thus, specific requirements are set out for equipment and protective systems of specific fields of use.

In order to apply this principle, the Ex dangerous areas others than mine undergrounds and those parts of surface mines that could be endangered by grizu firedamp mixture are divided into zones according to the likelihood and duration of an explosive atmosphere (Zones 0, 1 and 2 for gas and Zones 20, 21 and 22 for combustible dusts in air) and equipment is divided into categories according to the level of protection assured by avoidance of ignition sources during normal operation, during foreseeable malfunctions or during rare malfunctions.

Equipment in the ATEX field is divided into groups and categories as follows [1].

Table 1

Explosion group	Equipment category acc. ATEX Directive	Acc. new regulations (standard series: ISO 80079, EN 60079)
Group I (mining)	M1	
	M2	
Group II (A, B, C) Gas, vapors, mists - surface	1G	
	2G	
	3G	
Group II dusts	1D	Group III (A, B, C) dusts and fibers
	2D	
	3D	

The new standards have introduced the term level of protection of the equipment (Equipment Protection Level: Ga, Gb, Gc - for equipment intended for use in potentially explosive atmospheres generated by gas, and Da, Db, Dc - for equipment intended for use in potentially explosive atmospheres generated by combustible dusts in air) as equivalent to ATEx categories (1G, 2G, 3G).

Starting from the explosion protection principles above stated, in the following table are resumed the requirements for equipment according to its intended use.

Table 2

ZONE	Presence of explosive atmosphere	Ignition sources avoidance	evel of protection require	Group II cate-gory	EPL
2	Accidentally or only on a short period of time	During normal operation	NORMAL	3G	Gc
1	Likely to occur during normal operation	During foreseeable malfunctions (one fault)	HIGH	2G	Gb
0	Continuously, on long periods of time or frequently	During rare malfunctions (two independent faults)	VERY HIGH	1G	Ga
USERS		**MANUFACTURERS**			
European Directive 1999/92/EC (GD no. 1058/2006)		European Directive 94/9/EC (Government Decisions GD: no. 752/2004, no. 461/2006).			

Until recently both equipment for explosive atmospheres generated by gas and the ones generated by combustible dusts were included in Group II. The new specific standards have separated the equipment for environments with combustible dusts in Group III.

The conveyor belts, according to European Directive 94/9/EC represent components "U". As any other component, it has to be comprised in an equipment or protective system by its manufacturer / user, taking into account the manufacturer instructions [1].

Aiming to place it on the market, the conveyor belt have to fulfill the applicable essential safety and health requirements, supplemented with the technical and constructional requirements. In order to fulfill the applicable essential safety and health requirements, the conveyor belt shall be designed and manufactured following a risk analysis regarding the possibility of igniting explosive mixtures by its intrinsic ignition sources.

The following hazards have to be taken into consideration when analyzing the risks generated by the conveyor belt itself regarding its intrinsic ignition sources.

- electrostatic energy build up / discharges that may ignite the flammable atmosphere or may induce electric shocks to personnel;

- local heating by friction, due either to a driven rotary motion and a blocked belt, or a blocked drive and a moving belt, which might ignite the belt or the flammable atmosphere or the combustible dust;
- ignition of a conveyor belt by a small heat source as an open flame, blocked rollers or friction between belt and supports or support adjacent structure;
- flame propagation along a belt in fire. This ignition may be caused by a local small source as roller overheating or by a much more intense fire fed by other equipment or materials in the mine working. The fire amplitude increase together with the surrounding rocks temperature and pressure, with the length of the evacuation way and in case when there is a high amount of plastic materials in the mine working.

Once these dangers had been identified, each of them may be assessed in a satisfying manner based on laboratory tests performed according to standardized methods provided in series standards (SR EN 1554:2012, SR EN ISO 284:2013, SR EN 12881-1:2014, SR EN ISO 340:2013) [4], [5], [6], [7].

In order to ensure an acceptable protection level against these dangers, as soon as when designing and manufacturing the conveyor belt, choosing and selecting component materials is taken into consideration, to be able to grant different protective performances to the conveyor belts.

Thus, according to its intended use and protection performances provided, the specific standards (SR EN 12882:2009, SR EN 14973:2008) address several classes / categories of conveyor belts [2], [3].

Certification of conveyor belts as an ATEX component assumes attesting the protective performances to burning, burning propagation and static electricity.

When the conveyor belt is integrated into a belt conveyor that have to assure a certain protection level according to its intended use, if required, may need certain additional protective measures.

Additional protective devices refer to detecting dangerous situations and alarming or automatic stopping the conveyor. If need be, as provided in SR EN 620:2011, conveyors may be provided with the following types of automatic malfunction detection devices, to lower the hazards:

- belt decentration detection devices;
- conveyor, chutes, hoppers overload/blockage detection devices;
- shafts rotation detectors;
- belt velocity surveillance devices;
- thermal detectors;
- height and / or width detectors.

Belt conveyor conformity assessment with the essential health and safety requirements provided in the European Directive ATEX implies an explosion risk assessment that have to take into account potential ignition sources that may occur during normal operation and also during foreseeable malfunction and rare malfunction [11].

In practice two cases may be encountered, as follows:

- the conveyor, as a whole, as an assembly of several components, is placed on the market by a manufacturer, situation when the manufacturer has to perform the risk analysis which will be part of the technical file; he also has to assess product conformity with the ATEX requirements by applying applicable procedures according to product category.
- the conveyor is assembled or upgraded by user by assembling conveyor's already certified components. In this case, responsibility for ignition risk assessment incumbent on the user, who shall assume the manufacturer's obligations and responsibilities and it will be comprised either in the self-assessment technical file when the user is considered as manufacturer, or in the safety and health Document (see the Explosion Protection Document - directive 1999/92/CE), as applicable.

3. CONVEYOR BELT CONFORMITY CERTIFICATION WITH THE ATEX DIRECTIVE REQUIREMENTS

The 94/9/CE directive, transposed in Government Decision - GD no. 752/2004 and GD no. 461/2006 *concerning the conditions for placing on the market of equipment and protective systems intended for use in potentially explosive atmospheres* regulates equipment manufacturers obligations regarding conformity assessment according to category, see figure 1.

The previously mentioned modules describe the procedure by which the manufacturer ensures and declares his equipment or protective system is in conformity with the requirements of the 94/9/CE directive, transposed in GD 752/2004 and GD 461/2006. These procedures are founded on conformity assessment of equipment or protective system with the 94/9/CE directive; the difference between procedures is that in case of the procedure of *internal control of production* assessment is performed by the manufacturer as first-party assessment (self-certification), and in case of the procedure of *EC product unit verification* assessment is performed by a notified body as a third-party assessment/certification [1].

The declaration of conformity and the supportive technical documentation that have to be drawn up by the manufacturer are essential for conformity attestation with the specific requirements in the regulated field.

The content of declaration of conformity and technical documentation is given in the directive. Moreover, in order to clarify the issues, especially in case of product self-certification, the following standards had been drawn up: *SR EN ISO/CEI 17050-1 Conformity assessment. Declaration of conformity issued by the provider. Part 1: General requirements* and *SR EN ISO/CEI 17050-2 Conformity assessment. Declaration of conformity issued by the provider. Part 2: Supportive documentation.*

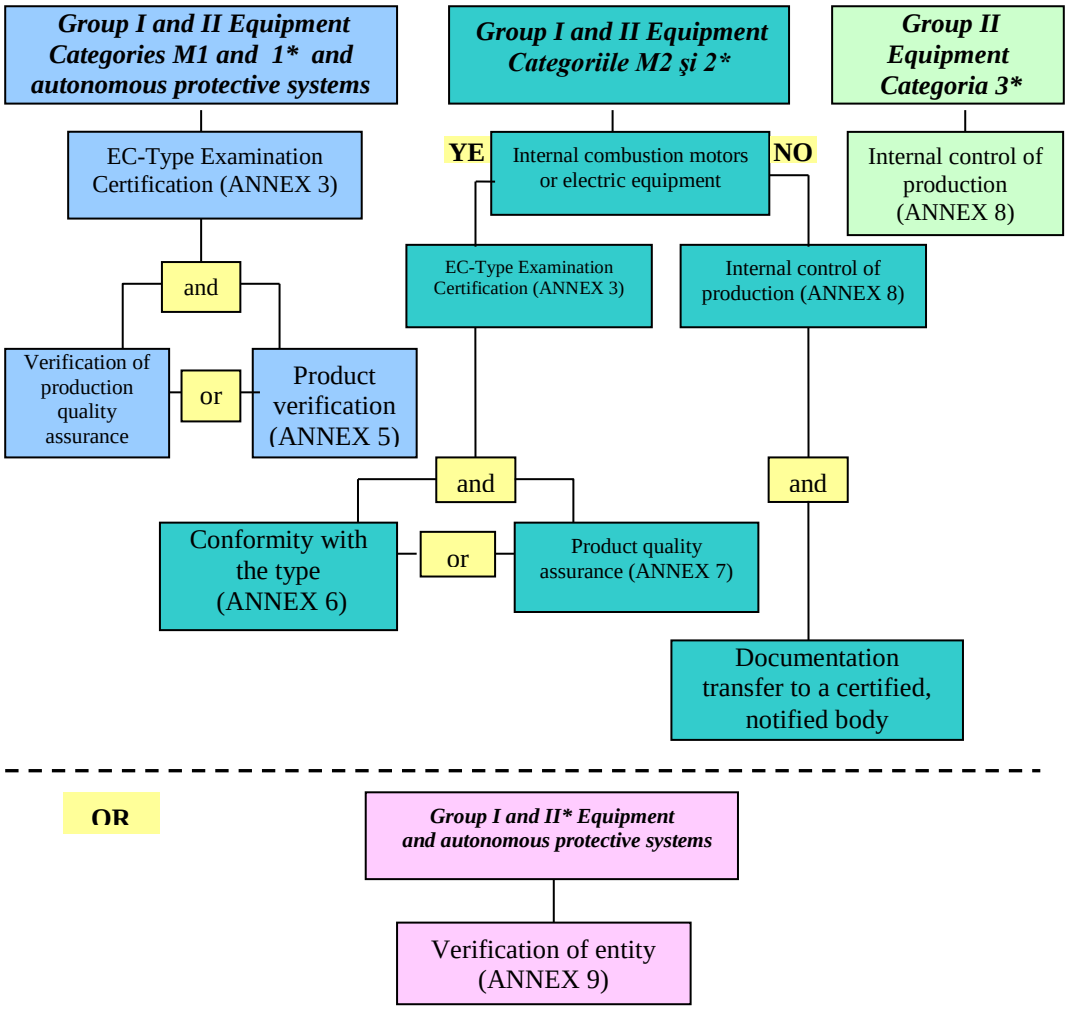

(*) and their components if these had been individually certified

Fig. 1 - The logic diagram of conformity assessment for equipment, components and protective systems

4. CONCLUSIONS

The conveyor belt, as component to be incorporated into an equipment (conveyor) with its intended use in environments with potentially explosive atmospheres shall fulfill the essential safety and health requirements regarding explosion prevention and protection.

In order to assess conveyor belt conformity with the applicable safety requirements, laboratory tests are required, as provided in the applicable standards.

Assessment for conformity certification of conveyor belts with the ATEX directive requirements is particularly important having in view the existing explosion hazard that has to be minimized in order to ensure safety of human life and health and to prevent goods and environment damage, as well as for a free circulation of products when they fulfill the essential safety requirements on European level.

For the purpose of ensuring a high safety level against explosions, additional to ignition hazards showed by conveyor belts, belt conveyors used in these environments and their components have to be submitted to a well documented official risk analysis, that should identify and list all potential ignition sources in the equipment and the measures to be applied in order to prevent potential ignition sources from becoming efficient.

REFERENCES

[1]. Directive 94/9/EC of the European Parliament and the Council of 23 March 1994 *on the approximation of the laws of the Member States concerning equipment and protective systems intended for use in potentially explosive atmospheres*.

[2]. SR EN 12882:2009, *Benzi de transport de uz general. Cerinţe de securitate electrică şi de protecţie împotriva inflamabilităţii.*

[3]. SR EN 14973 + A1:2008, *Benzi transportoare pentru utilizare în instalaţii subterane. Cerinţe de securitate electrică şi de inflamabilitate.*

[4]. SR EN 12881-1:2014, *Benzi transportoare. Încercări de simulare a inflamabilităţii. Partea 1: Încercări cu arzător cu propan.*

[5]. SR EN 1554:2012, *Benzi transportoare. Încercări la frecare ale tamburului*.

[6]. SR EN ISO 340:2013, *Benzi transportoare. Caracteristici de inflamabilitate la scară de laborator. Cerinţe şi metodă de încercare*.

[7]. SR EN ISO 284:2013, *Benzi transportoare uşoare. Conductibilitate electrică. Specificaţie şi metodă de încercare*.

[8]. Lupu, L., Proiect program NUCLEU *„Dezvoltarea metodelor de evaluare pentru instalatiile de transport cu banda destinate utilizării în minele subterane grizutoase – echipament neelectric de grupa I – METBEN”*, 2010-2011.

[9]. Păun F.A., Proiect Program NUCLEU *„Dezvoltarea facilităţilor de cercetare privind riscul sau frecvenţa probabilă de producere a unor fenomene periculoase în funcţie de circumstanţele specifice ale aplicaţiilor din atmosfere cu pericol de explozie a benzilor transportoare (DFCBT)”*, 2010-2011.

[10.] Păun F.A., *Proiect Program NUCLEU, faza V/2012 „Tehnologie pentru încercarea benzilor transportoare la ardere la scară mică în conformitate cu standardul european”*, 2012.

[11]. Părăian M., Ghicioi E., Burian S., Aspects regarding conformity assessment or self-assessment for products used in potentially explosive atmospheres with the safety requirements of explosion prevention.

Annals of the University of Petrosani, Electrical Engineering, 17 (2015)

MODERN METHODS OF REACTIVE POWER COMPENSATION AND REDUCTION OF SUPERIOR CURRENT AND VOLTAGE HARMONICS

MARIUS DANIEL MARCU[1], TITU NICULESCU[2], FLORIN-GABRIEL POPESCU[3], RAZVAN SLUSARIUC[4]

Abstract: Active power filters (FAP) adapts to varying grid and load. The composition of active power filters are static converters, having inverters structure, operating in four quadrants. These inverters have the advantage of bi-directional energy transfer and exchange between the grid and a storage element, capacitive or inductive type, which is located on the D.C. part of the converter.

If it is used AS a centralized compensation solution it can combine power factor correction circuit with harmonic filter to solve more problems with the same equipment.

Keywords: active power filter, harmonics, compensation, inverter, reactive power.

1. REACTIVE POWER COMPENSATION

Current installations of reactive power compensation are affected by harmonics and most of the electricity companies recommend rules and some even prescribe as existing reactive power plants compensation to be filled with a coil. This means that the capacitor must be connected in series with a coil so that the circuit for the higher harmonics to behave as an inductive element, and the fundamental frequency to remain as a capacitive element [6].

[1] *PhD. Associate Professor Eng. University of Petrosani*
[2] *PhD. Associate Professor Eng. University of Petrosani*
[3] *PhD. Lecturer, Eng., University of Petrosani*
[4] *Ph.D. Assistant Eng., University of Petrosani*

When the inductive element is added intentionally installations are connected to the resultant voltage of the entire absorbant circuit. Overvoltages remain inside the compensation installation, it appears across the properly sized capacitor, but across the entire system there are no overvoltages.

It is important to remember that, especially when connected to a single-phase nonlinear load, for networks of 50Hz appear harmonics from 100 Hz to over 1 kHz, that gives a large field of resonances which can be excited.

2. ACTIVE POWER FILTER (APF)

Traditional methods for removal of harmonics based on plants resonant passive filters LC parallel source of harmonic and synchronized therewith is a rigid structure able to eliminate the defined harmonics, while in reality the content of harmonic loads connected to the network are unpredictable and variable in time. This leads to unwanted resonances between filters installed and line impedance that leads to overload or overvoltages in filters under load and installation in general [6].

The solution is to install filters that adapts to varying network and load that are called active power filters (APF) adequate installations containing static converters and control algorithms [8].

Active power filters is for the network a variable impedance with a value necessary to facilitate the elimination of harmonics. They are not based on a rigid structure and are suitable for complex waveforms, its description no being so simple.

As shown in Figure 1, the active filter is a shunt device. A current transformer measures the harmonic content of the load current and controls a current source to generate an exact copy of the current to be injected in the next period.

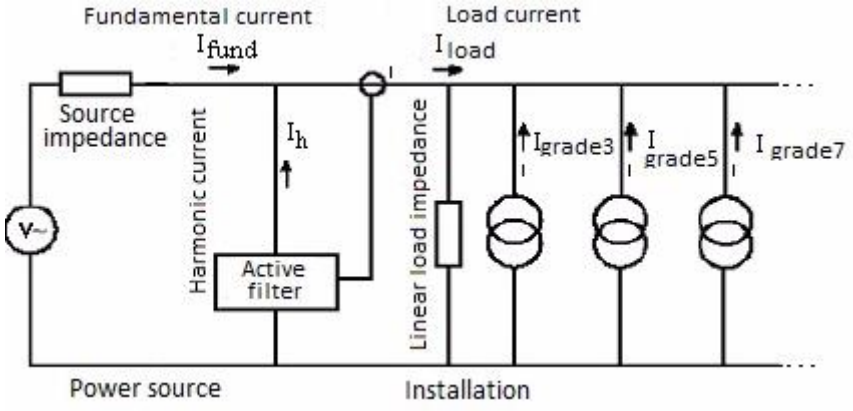

Fig. 1. Active power filter

Harmonic current is generated by the active filter and only the fundamental current is drawn from power grid.

In practice, the amplitudes of harmonic current are reduced by 90% and, because the impedance of the source at harmonic frequencies is reduced, voltage distortion is reduced.

3. COMBINED EQUIPMENT FOR COMPENSATION AND FILTERING

In practice, the functions of compensation of reactive power and filtering of the harmonic current are most often combined. It is usual to set the resonant frequency of the LC circuit at a frequency that does not correspond to harmonics to avoid overloading the compensation system. Sizing the coil is normally made as a percentage of reactive power of the capacitor at 50 Hz.

For example, for a variance of 5%, which is a voltage drop across the inductor 1/20 and 21/20 voltage drop across the capacitor so that the resulting decrease in total 100%. For a frequency of 20 times greater, so 1000 Hz, the relationship is reversed; this frequency the two identical impedance elements present, and the resonance frequency of the circuit is apparent that the geometric mean of the two frequencies, that is, the value:

$$50\,Hz \cdot \sqrt{20} = 224 \quad Hz \tag{1}$$

Another common value, 7%, determines a resonant frequency of 189 Hz avoids the appearance of a cage for a close harmonic. Because the LC is connected to the electrical network, harmonics from external sources can flow through it simultaneously with the internal sources for which it has been designed. Therefore, if a consumer uses a filter but those next to him does not, you need to oversize the filter [1], [4], [5].

In some cases, oversizing will not only avoid unforeseen overload but also improve the filter quality factor, providing a more precise separation desired from the undesired frequencies with reduced energy losses. This effect is reduced if the unit is separated from the others by a distribution transformer, with the corresponding the inductivity.

Active filters (APF) are normally connected in parallel with the network. But the situation is quite different. These electronic devices analyze nonlinear harmonic current on the consumer and generates exactly deforming residue in the future. In this way, the residue is provided by deforming the active filter, and the current fundamental is taken from the power grid. If the residual current is above the filter capacity, then it

only partially achieved the necessary correction and some current harmonics are taken from the network [7].

4. SIZING THE INVERTER OF THE ACTIVE FILTER

Static converters used in FAP have structure inverters operating in four quadrants, with the ability to transfer and exchange between the network and a bidirectional energy storage element, capacitive or inductive type, located on the D.C. converter.

In figure 2 are shown the structures of the three converters commonly used in the version of three-phase network without neutral.

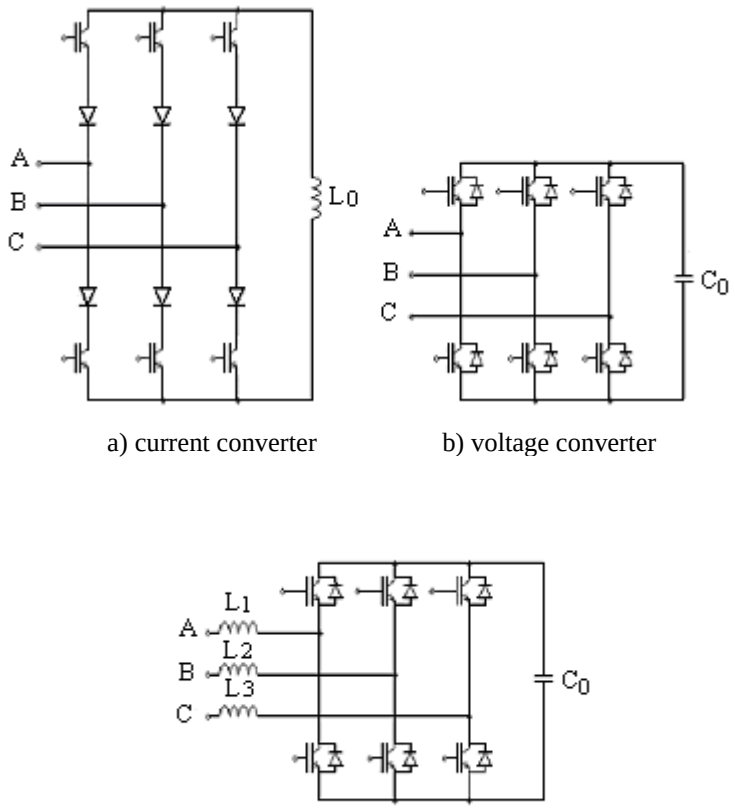

a) current converter b) voltage converter

c) voltage converter in current adjustment mode

Fig. 2. Current converter, voltage converter, voltage converter in current adjustment mode

The voltage converter in adjustment mode after inserting an inductance between network and converter so that the entire system behaves as a current source.

The voltage inverter is made with IGBT, which gives him the advantage of simplicity diagram of force because it no longer requires auxiliary circuits of extinction as thyristor the variants, blocking transistors being made through the gate.

Control methods in the time domain to obtain instantaneous values are based on control signals required for compensation.

There are methods that have been used mainly in 1990, starting from the first Theory of Instantaneous Reactive Power to control FAP introduced by Akagi et al in 1983 [2], [3] which has had significant success for elimination harmonic in the presence or not of reactive power in the conventional sense.

During these last years we have developed other methods in the time domain, highlighting the advantages for control of FAP [10].

All these methods are obtained compensation currents but not voltages because they are very suitable for FAP structure that acts as a current source in parallel with the network.

Load currents must be analyzed to obtain compensation currents. Fundamental active current is calculated and subtracted from the load current. The resulting current is denied to obtain the reference current to the active filter. Load current fundamental calculation is done using fast Fourier transform (FFT).

$$I_s(k) = \sum_{n=1}^{N} i_s(n) e^{-j2\pi(k-1)\left(\frac{n-1}{N}\right)} \qquad 1 \le k \le N \tag{2}$$

in which:
k - order harmonic
n - sample order
AND - load current
is (n) - n sample from the load current
N - number of samples

Calculating the inverse Fourier transform (IFFT) to obtain fundamental active current task in domain of time. The equation is the inverse Fourier transform:

$$I_s inv(n) = \sum_{k=1}^{N} I_s(k) e^{j2\pi(k-1)\left(\frac{n-1}{N}\right)} \qquad 1 \le k \le N \tag{3}$$

Because the data entered into the calculation of the inverse Fourier transform and not imaginary part, the data they will have no imaginary part, it is sufficient only recreating real part of the samples.

Now reference currents, which are supposed equal to those of the reaction can be calculated using the formula:

$$i_f(n) = -\left[i_f(n) - i_s inv(n)\right] \qquad 1 \le k \le N \tag{4}$$

4.1. Calculation of the filtering coil

Maximum ripple current is the main criterion in the design chosen coil filtering. Ripple current calculation is made on the assumption lack of load and the effect coil resistance is neglected. In these circumstances the reference voltage of the inverter is equal to the supply voltage. The value peak to peak ripple current is:

$$\hat{i}_{riplu} = \frac{m \cdot u_{cc}}{8 \cdot \sqrt{3} \cdot f_{com} \cdot L_f} \tag{5}$$

where:
u_{CC} - the value of the DC voltage
f_{com} - switching frequency

And closed loop systems in the absence of load, the controller aims modulation factor to:

$$m = \frac{2\sqrt{2} \cdot U_s}{u_{cc}} \tag{6}$$

where:
Us - the effective value of the phase voltage

Inductance required is calculated by formula (7) it is assumed ripple current up to 15% of rated current:

$$L_f = \frac{U_s}{2\sqrt{6} \cdot f_{com} \cdot \hat{i}_{riplu}} = \frac{230}{2\sqrt{6} \cdot 10^4 \cdot 32{,}26} = 0{,}145[mH] \tag{7}$$

For ripple current 32.26 [A] peak to peak (15% of current compensation) is required inductance of 0.145 [MH].

It notes that the inductance value depends on the maximum ripple current and voltage required for closed-loop systems. Closed loop systems due to switching the inverter voltage harmonics are not directly proportional DC voltage.

4.2. The calculation of the reference voltage of active filter

To calculate minimum DC voltage must first calculate the required voltage of the active filter. Required active filter voltage can be calculated as:

$$u_f^* = u_s - L_f \cdot \frac{di_f}{dt} \tag{8}$$

The advance 1.5 current sampling period is calculated using the converter current samples which are in advance by two, respectively one sampling step like in the relation:

$$\frac{di_f}{dt}(n) = 2 \cdot f_{com} \cdot \left[i_f(n+2) - i(n+1) \right], \qquad 1 \le n \le N \tag{9}$$

4.3. Choosing DC voltage

Assuming modulation with a space phasor the required continuous voltage is given by the following:

$$m_{\max} \cdot \frac{2}{\sqrt{3}} \cdot \frac{u_{cc}}{2} > u_{ref\,\max} \tag{10}$$

$$u_{cc} = \frac{\sqrt{3} \cdot u_{ref\,\max}}{m_{\max}} = \frac{\sqrt{3} \cdot 348}{0.95} = 635\,[\mathrm{V}] \tag{11}$$

For a maximum modulation index of 0.95 obtain maximum continuous voltage of 635 [V] is rounded to 650 [V]. Also voltage can be slightly higher when taking into account sags, voltage transducer accuracy etc.

In the calculations above the ripple current was taken to 15% of peak current compensation. Actual value of ripple current through the coil filter with a phasor spatial modulation in no-load approximates with the relation:

$$I_{Lriplu} = \frac{u_{cc} \cdot M}{8\sqrt{3} \cdot L_f \cdot f_{com}} \cdot \sqrt{0.5 - 0.735 \cdot M + 0.35 \cdot M^2} \tag{12}$$

where:

$$M = \frac{2\sqrt{2} \cdot U_s}{u_{cc}} = \frac{2\sqrt{2} \cdot 230}{650} = 1 \tag{13}$$

$$I_{Lriplu} = \frac{650 \cdot 1}{8\sqrt{3} \cdot 0.000145 \cdot 10000} \sqrt{0.5 - 0.735 \cdot 1 + 0.35 \cdot 1^2} = 9{,}94\,[\text{A}] \tag{14}$$

With the help of expression (12) ripple current through the coil is 9.94 [A].
The total effective current including the ripple is given by the following:

$$I_{TOTbob} = \sqrt{I_{comp}^2 + I_{riplu}^2} = \sqrt{121{,}68^2 + 9{,}94^2} = 122{,}09\,[\text{A}] \tag{15}$$

4.4. Calculating DC

With the help compensation voltages and currents we can calculate the DC using the expression:

$$i_{cc}(n) = \frac{u_{f1}(n) \cdot i_{f1}(n) + u_{f2}(n) \cdot i_{f2}(n) + u_{f3}(n) \cdot i_{f3}(n)}{u_{cc}}, \qquad 1 \le n \le N \tag{16}$$

4.5. Calculating capacitor

The capacitor is calculated to limit the peak to peak ripple value to a certain percentage of the nominal voltage relation:

$$C = \frac{\left(\int i_{dc} dt\right)_{vv}}{u_{cc_{VV}}} \tag{16}$$

Peak to peak ripple value of the integral direct current is 0.48 A-sec. In order to limit this value to 5% of the supply voltage is 650 [V], the capacitor must have a capacity of 14.8 [mF] As is shown from the following relation:

$$C_{calc} = \frac{0.48}{0.05 \cdot 650} = 14{,}8\,[\text{mF}] \tag{17}$$

5. CONCLUSIONS

There are few common devices that the most effective way of reactive power compensation is on-site. This solution is the most efficient because only the active component of current flows in the system, the reactive component is compensated inside the device.

The advantage of the solution centralized with the appropriate control, is that not all devices operate simultaneously and it is possible, many times to install a total capacity of offset less than if it would provide compensation for the local all equipment. It thereby reduces the risk of overcompensating motors. Using a combination of filter and compensation reduces the risk of resonance and ensures that the filter harmonics within the range are mitigated.

The composition of active power filters are static converters, having inverters structure, operating in four quadrants. These inverters have the advantage of bi-directional energy transfer and exchange between the grid and a storage element, capacitive or inductive type, which is located on the D.C. part of the converter.

The calculations are needed to help determine active filter inverter constructive solutions to meet the filtration system.

Because of these possibilities, static converters can be implemented for single-phase or three-phase systems with or without neutral. In all these cases, the static converter can act as a current source or voltage source, ie as an energy storage element used. The structure most often used in these situations is found in three-phase systems in two versions, namely for systems with and without neutral.

REFERENCES

[1]. **Abellan A., Benavent J. M.**, *A new combined control method for shunt active filters applied to four-wire power systems,* EPE 2001 – Graz, 2001.

[2]. **Akagi H., Kanazawa Y., Nabae A.** *Generalized theory of the instantaneous reactive power in three-phase circuits,* Proceedings of IEEJ International Power Electronics Conference (IPEC-Tokio), Pages: 1375-1386, 1983.

[3]. **Akagi H., Kanazawa Y., Nabae A.**, *Instantaneous reactive power compensators comprising switching devices without energy storage components*. IEEE Transactions on Industry Applications, Vol. IA-20, No. 1, Pages: 625-630, May/June 1984.

[4]. **Aredes M., Watanabe E. H.**, *New control algorithms for series and shunt three-phase four-wire active power filters*, IEEE Transaction on Power Delivery, Vol. 10, No. 3, 1995.

[5]. **Fujita H., Akagi H.**, *The unified power quality conditioner: the integration of series and shunt-active filters*, IEEE Transactions on Power Electronics, Vol. 13, No. 2, 1998.

[6]. **Golovanov C., Albu M.**, *Probleme moderne de măsurare în electroenergetică*, Editura Tehnică, Bucureşti, 2001.

[7]. **Marcu M.D., Popescu F.G., Niculescu T., Pana L., Handra A.D.,** *Simulation of power active filter using instantaneous reactive power theory*. Harmonics and Quality of Power (ICHQP), IEEE 16th International Conference, Page(s):581 – 585, Bucharest, Romania, 25-28 May, 2014.

[8]. **Marcu M.D., Popescu F.G., Pana L.,** *Modeling and simulation of power active filter for reducing harmonic pollution using the instantaneous reactive power theory*. Environmental Engineering and Management Journal, June 2014, Vol.13, No. 6, Pages: 1377-1382.

[9]. **Popescu F.G., Arad S., Marcu M.D., Pană L.,** *Reducing energy consumption by modernizing drives of high capacity equipment used to extract lignite*, Papers SGEM2013/Conference Proceedings, Vol. Energy and clean technologies, ISBN 978-619-7105-03-2, 183 - 190 pp, Albena Co., Bulgaria , 2013.

[10]. **Tolbet L.M., Habetler T.G.**, *Comparison of time-based non-active power definitions for active filters*, CIEP, Acapulco, MEXICO, Pages: 73-79, October 15-19, 2000.

[11]. **Uţu I., Samoilă L.,** *Măsurarea mărimilor electrice,* Editura Universitas, ISBN 978-973-741-162-4, pp. 256, Petroşani, 2010.

[12]. **Uţu I.,** *Reduce the harmonics from mining extraction plants operated with DC motors*, Proceedings of the12th International Conference on Instrumentation, Measurement, Circuits and Systems (IMCAS '13), Kuala Lumpur, Malaysia, ISBN: 978-1-61804-173-9, pag. 24-28, 2013.

Annals of the University of Petrosani, Electrical Engineering, 17 (2015)

THE IGNITION SENSITIVITY OF GASEOUS EXPLOSIVE ATMOSPHERES FROM THE UNDERGROUND OF FIREDAMP MINES DUE TO AIR MOISTURE

MARIUS DARIE[1], SORIN BURIAN[2], TIBERIU CSASZAR[3], LUCIAN MOLDOVAN[4], COSMIN COLDA[5], CLEMENTINA MOLDOVAN[6], ADRIANA ANDRIŞ[7]

Abstract: This paper presents an investigation by statistical analysis of the influence of humidity on the ignition sensitivity of explosive gas atmospheres in the underground of firedamp mines from the low current equipment and installations.

The first part briefly describes the test rig used and the results obtained from experimentation.

Because of the stochastic behaviour of the results there were used statistical methods of analysis.

The second part presents statistical analysis of experimental results obtained from tests with explosive mixture of air-methane.

The third part presents the resulted theoretical model.

Keywords: firedamp mines, explosive atmospheres, ignition sensitivity, humidity.

1. Introduction

The process of coal mining by using underground mine works is constantly accompanied by the risk of explosion due to the presence of methane and coal dust, released into the atmosphere from underground during the extraction of coal.

[1] *Ph. D.Eng., scientific researcher II, INDC-INSEMEX Petroşani*
[2] *Ph. D.Eng., scientific researcher II, INDC-INSEMEX Petroşani*
[3] *Ph. D.Eng., scientific researcher II, INDC-INSEMEX Petroşani*
[4] *Ph. D.Eng., scientific researcher III, INDC-INSEMEX Petroşani*
[5] *Ph. D.Eng., scientific researcher III, INDC-INSEMEX Petroşani*
[6] *Lect. Ph. D.Chim., University of Petroşani*
[7] *Eng., scientific researcher , INDC-INSEMEX Petroşani*

Considering the classifications of explosive atmospheres one can say that the atmosphere in the underground of firedamp mines has the highest ignition threshold, whether it takes into account the electrical criteria (260 μJ) or the thermal criteria (450°C).

Experimental study of the probability of ignition [4] revealed an approximately exponential dependence [2] of the probability of ignition depending on voltage, in capacitive circuits. Other mentions [5] presents an exponential dependence of the ignition probability depending on the logarithm of the current value, in inductive circuits.

Another concurrent factor influencing the sensitivity to ignition of underground atmospheres, characterized by the presence of methane, is its humidity content.

On the other hand, the phenomenon of explosion propagation in areas characterized mainly by one-dimensional development involves pre-compression phenomena and increase the speed of propagation of the explosion wave front and leads to events of very high gravity that includes both casualties and material losses.

Additionally, an explosion causes in the underground damage to ventilation system that has cascading consequences in terms of reducing the capacity of exhausting the methane emissions and also decreasing the capacity of providing the required oxygen level to the workers caught in the associated underground mine works [1].

Experimental study of the dependence of ignition sensitivity of methane explosive atmospheres against humidity showed a slight linear relationship to the logarithm of the number of rotations at which the ignition of the test mixture has occurred [3].

2. Brief presentation of experimental data

Experimentation was carried out using the test infrastructure for ignition by spark (spark test apparatus). A chamber, that contains a transducer, has been additionally connected at the air intake for measuring environmental parameters including humidity.

An 8,3% air-methane test mixture was used and having the relative humidity of the air at the intake between 11 ÷ 38% RH.

The electric parameters of the circuit in which the spark test apparatus has been connected were Uo=24Vcc, L=121mH, Io=110÷111mA.

During the performance of the test the inlet air humidity varied according to the diagram in Figure 1 and the value of the number of rotations at which the ignition occurred is shown in the diagram in Figure 2.

The procedure for conducting the experiments included successively:

- conditioning of spark test apparatus according to B.1.3 in [5] at the beginning of the test series then;

- cycles of 15 tests conducted as follows:
    - purging with air of the transducer chamber for a period of between 4 to 10 minutes;
    - purging the chamber of the spark test apparatus and related gas ducts with 10 volumes of mixture;
    - starting the spark test apparatus with specified electrical parameters;
    - recording the number of revolutions to which the ignition has occurred;
    - reading the indicated value for the intake air humidity and recording, in an identical manner, for all the tests in the cycle. The reason is to allocate the time needed to stabilize the humidity value indication of the device.

For the first 140 tests the time needed to stabilize the instrument indication wasn't booked, that is the reason why these were dropped-out (on the left of the line) - see Figure 1.

Although the conditioning of the cadmium disk was performed, on the first 60 tests an anomaly was found in the distribution of the number of rotations values at which the ignition had occurred. See Figure 2.

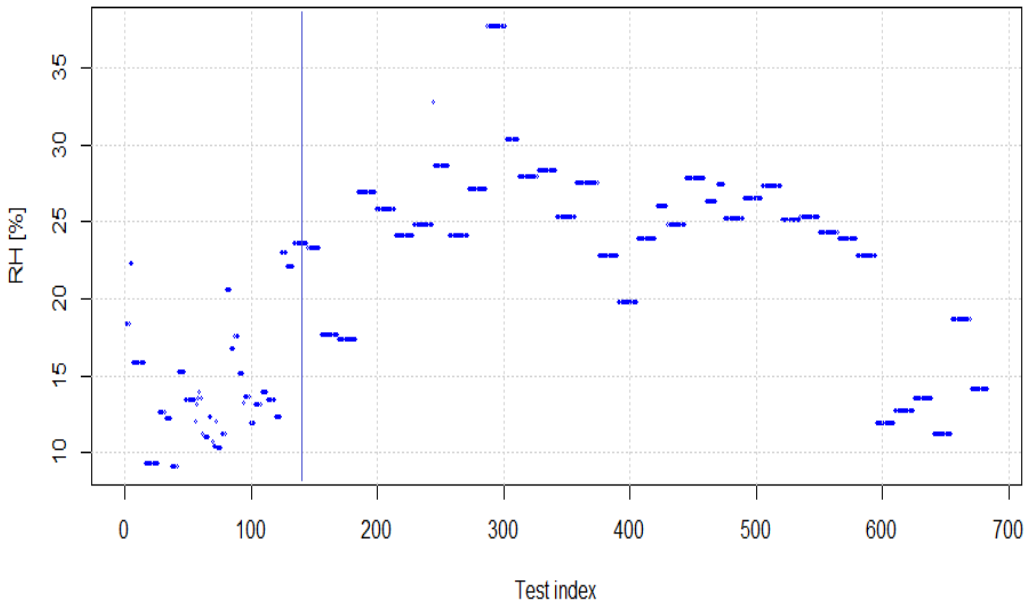

Fig. 1. Variation of the intake air humidity

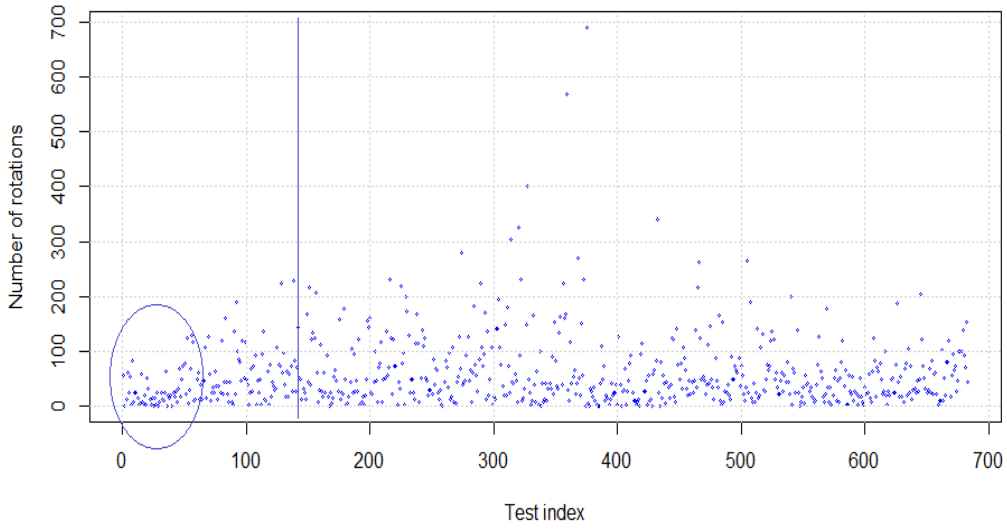

Fig. 2 The number of rotations at which the ignition occurred

Distribution of values of the air relative humidity at the inlet and of the number of rotations at which the ignition has occurred is shown in the diagrams in Figures 3 and 4.

After removing the first 140 tests from the initial set of experimental data the density distribution diagram was built - Figure 5.

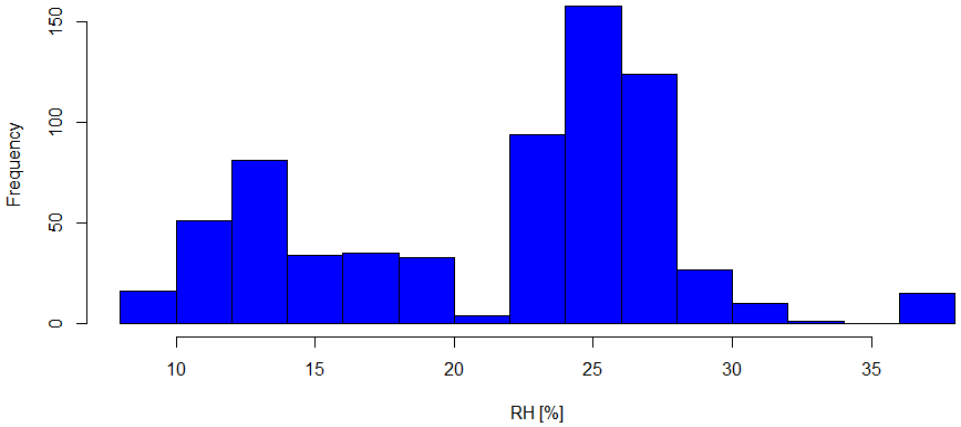

Fig. 3 The histogram of values of air relative humidity at intake

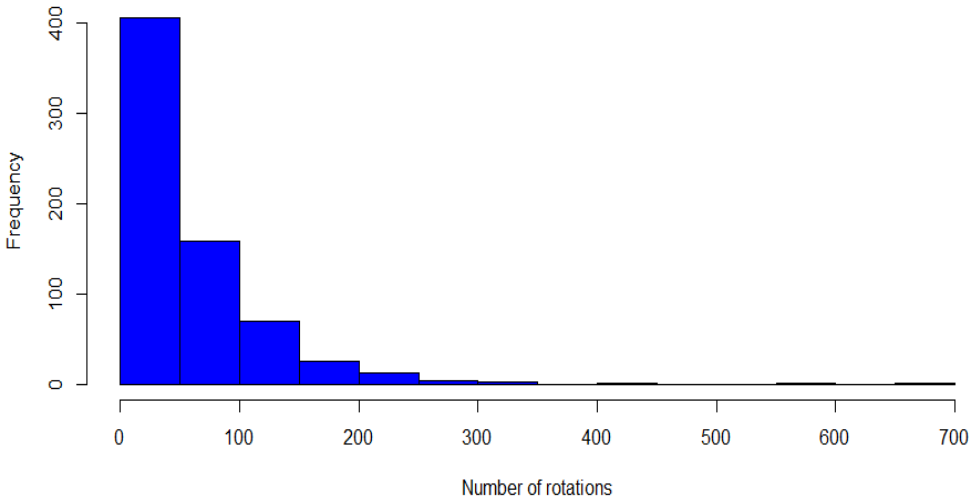

Fig. 4 The histogram of the number of rotations at which the ignition has occurred

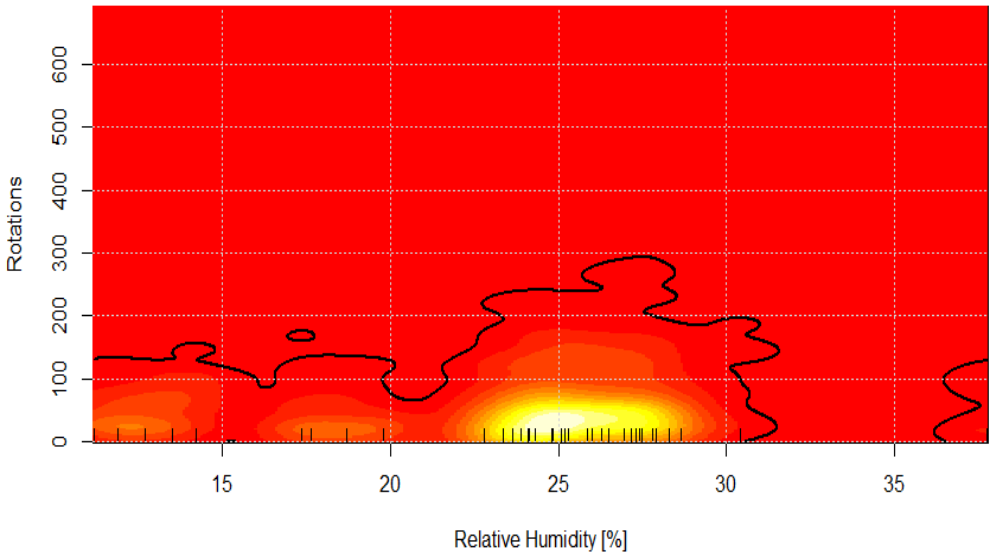

Fig. 5 Distribution of density for the number of rotations at which the ignition occurred and relative humidity of air at intake

3. Preliminary statistic test

The set of results was divided in two series, one with the air relative humidity at intake smaller than 21 % RH and the other with higher relative humidity.

Application of the statistical test for the two series showed application of Student test for the two series showed that the difference between the arithmetic mean of rotations for the two sets is statistically significant - is between 5.75 ÷ 26.40 (means 50.16729 and 66.24389 rotations) with a confidence level of 95%.

4. Theoretical model of transformation

In order to highlight the influence of the air relative humidity at the intake on the ignition sensitivity for normalization of rotation values at which the ignition has occurred, the function in equation (1) was proposed, based on the combination of logarithm function with the CoxBox transformation.

$$T(x,\lambda) = \frac{(ln(x))^{\lambda}-1}{\lambda} \quad (1)$$

In equation (1) the λ parameter is a coefficient and its value is determined by an optimization process that reduces the value of the objective function proposed in equation (2).

$$F(X,\lambda) = \left(skewness\left(T(X,\lambda)\right)\right)^4 + \left(3 - kurtosis\left(T(X,\lambda)\right)\right)^2 \quad (2)$$

In equation (2) X represents the vector of rotations values at which the ignition has occurred and λ represents the argument of the optimization function.

Following the application of the optimization process a value of 1.303125 for λ has resulted.

Then the function defined in equation (1) applied on the rotation vector values to which the ignition has occurred.

The histogram of the converted values of rotations at which the ignition has occurred together with the empirical density distribution curve and the theoretical density curve (Gauss) are shown in the diagram in Figure 6 and QQ plot in Figure 7.

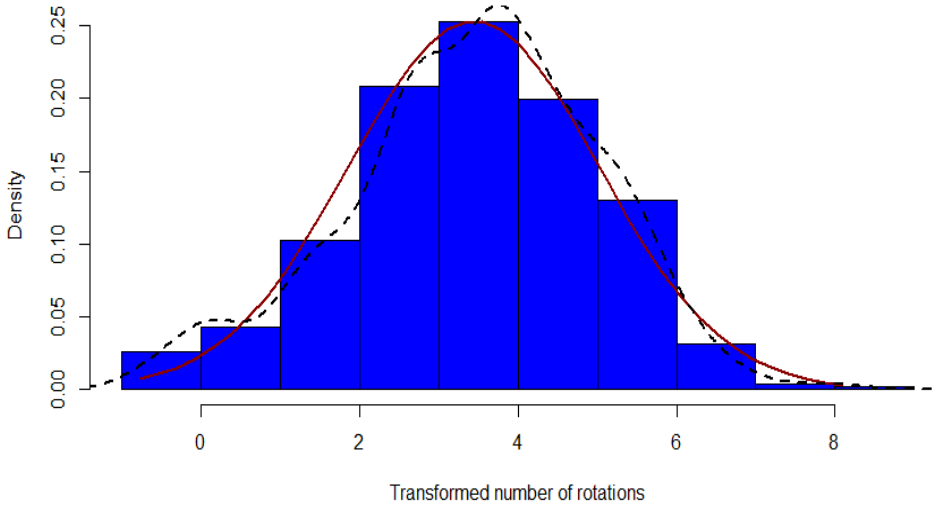

Fig. 6 The histogram of converted values of rotations at which the ignition has occurred

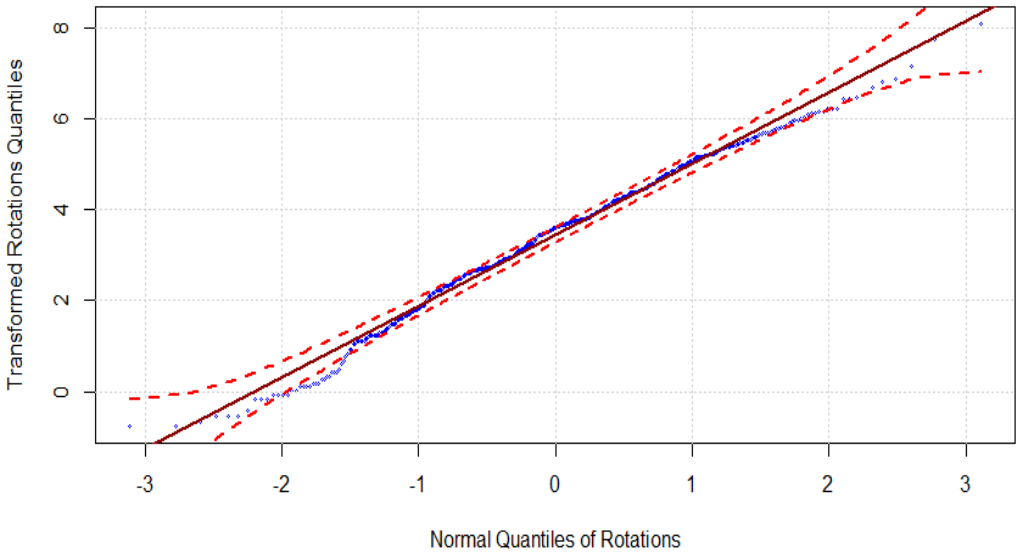

Fig. 7 QQ diagram of values for rotations transformation to normal distribution (Gauss)

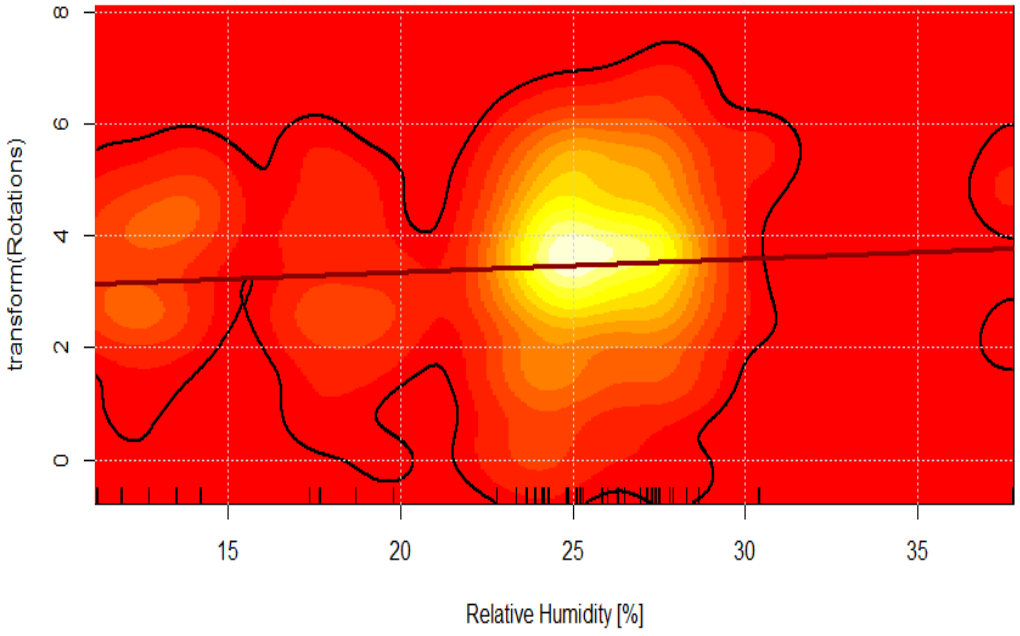

Fig. 8 Distribution density of the transformation of the rotations number at which the ignition has occurred and the relative humidity of the air at the inlet

On the density diagram of experimental points the transformation of rotation versus the relative humidity of air at intake the regression line was drawn whose slope is observed that is slightly positive. See Figure (8).

Application of Student statistical test for the slope value of the diagram of rotation transformation depending on the air relative humidity at intake revealed that its value is in the range 0.0004697686 ÷ 0.04825771 with a confidence level of 95%. Also, the probability for the slope to be zero or negative is 0.6%.

Further, bootstrapping has been applied for the regression slope value of random subsets of values and distribution of slope values is shown in the diagram in Figure 9.

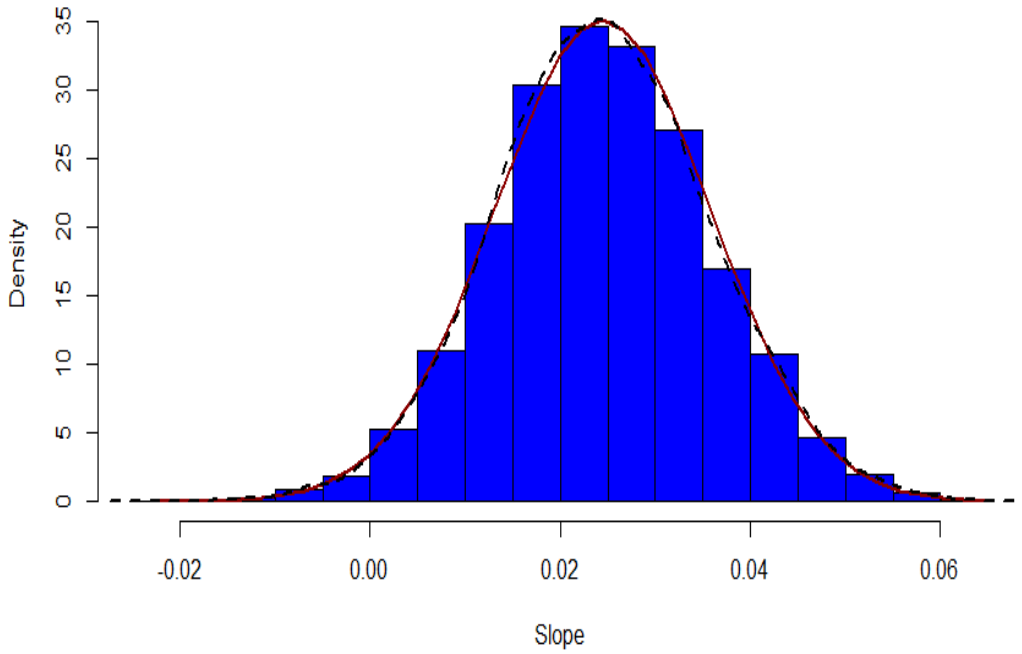

Fig. 9. Histogram of regression line slope values

5. CONCLUSIONS

1) Preliminary analysis of data resulting from experiments showed that there is a statistically significant difference between arithmetic mean of the number of rotations at which the ignition occurred for relative humidity of air at intake below 21% and those over 21%.
2) Due to the asymmetric shape of the distribution of rotation values at which the ignition of the test mixture occurred, the use of a transformation based on a combined logarithm function and Box-Cox was proposed.

3) In order to determine the λ parameter of the chosen transformation an objective function was proposed and used, which aims to reduce both asymmetry and excess kurtosis.
4) For the data set obtained after applying the transformation the regression line was determined and its slope was analysed.
5) Following statistical analysis of the slope of the regression line resulted that this has values greater than zero, with a probability of 99.4%.
6) Due to the large dispersion of values for the number of rotations at which the ignition has occurred, this paper failed to identify a dependency relationship to ignition sensitivity, but only established that the relative inlet air humidity significantly influences the sensitivity to ignition of 8.3% air + methane mixtures.

6. ACKNOWLEDGMENTS

This paper is based on experimental results emerged from National Research Program PN 07 45 01 41 conducted with support of ANCSI. For performing the calculus and diagrams were used the R language and R Studio environment [6, 7] along with the bootstrap [9, 10], moments [8], fitdistrplus packages and R script for contour and density plot [11].

REFERENCES

[1] Cioclea Doru, Artur George Găman, Ion Gherghe, Florin Rădoi,Corneliu Boantă, Vlad Pasculescu, *Possibilities to priorly establish the structures of ventilation networks affected by underground explosions*, The 24th International Mining Congress and Exhibition of Turkey, 14 – 17 April 2015, Antalya, Turcia, ISBN 978-605-01-0705-0, Pag. 991-997, 2015

[2] Darie M., Ionescu J., Burian S., Csaszar T., Moldovan L., (*2012), Ignition probability assessment of low current circuits designed for use in explosive atmospheres*, Environmental Engineering and Management Journal, volume 11/2012, No.5

[3] Darie M., Burian S., Ionescu J., Csaszar T., Moldovan L., Andriş Adriana (2014), *Air Humidity – a Significant Factor on Ignition Sensitivity of Gaseous Explosive Atmospheres*, Proceding of ELSEDIMA International Conference – 18 – 19 September 2014, Cluj-Napoca, Romania.

[4] Johansmeyer U., *(1994), Investigations into the Intrinsic Safety of field bus systems, PTB-Bericht.*

[5] Standard IEC 60079-11: 2012 - *Explosive atmospheres* -- Part 11: Equipment protection by intrinsic safety "i".

[6] R Development Core Team (2008). R*: A language and environment for statistical computing.* R Foundation for Statistical Computing, Vienna, Austria. ISBN 3-900051-07-0, URL http://www.R-project.org.

[7] R Core Team (2015). *R: A language and environment for statistical computing.* R Foundation for Statistical Computing, Vienna, Austria. URL http://www.R-project.org/.

[8] Lukasz Komsta and Frederick Novomestky (2015*). Moments, cumulants, skewness, kurtosis and related tests.* R package version 0.14. http://CRAN.R-project.org/package=moments

[9] Angelo Canty and Brian Ripley (2015). *boot: Bootstrap R (S-Plus) Functions. R package version 1.3-15.*

[10] Davison, A. C. & Hinkley, D. V. (1997) *Bootstrap Methods and Their Applications.* Cambridge University Press, Cambridge. ISBN 0-521-57391-2.

[11] Forester J.D. (2008) *Contour for plotting confidence interval on scatter plot of bivariate normal distribution,* URL https://stat.ethz.ch/pipermail/r-help/2012-March/305400.html.

Annals of the University of Petrosani, Electrical Engineering, 17 (2015)

THE RET DEVELOPMENT DUE TO ENERGETIC MIX IN THE ELECTRICAL ENERGY PRODUCTION

MARIA DANIELA STOCHITOIU[1], ILIE UTU[2]

Abstract: Energy is a product with great economic, social, strategic and political value. Main objective of Romania`s growth during the next decades is insurance of sustainable social and economic development conditions with cannot be designed without an appropriate strategy for energy transport structure (RET).

Keywords: sustainable development, energy markets, climate change, renewable energy sources

1.INTRODUCTION

The modern society shouldn't exist without a safety, clean and certain electrical energy supply as well as an affordable price. The electrical energy is one of the base conditions for economic and social development for education, health and all aspects of human life.

In the last twenty years, there were major changes in the electrical energy develop system meantime the electrical societies have relied their strategies on the predictable and stable conditions, the industry- which is still powerful regulated – is frequently putting face to face with frameworks of rules and climate regulations in nowadays [1].

These aspects have determined the world energy domains leaders to gather the Global Energy Initiative for sustaining and promote the electrical companies efforts for energy to assure a certain supply, to improve the access to energy and to reduce or to adopt the climate changes impact.

As specific particularities of energy sector, it can mention: a high inertia due to interval of time between decision and implementation; along with transport structure is main contributor to environmental pollution and climate changes; it needs important financial investments.

[1] *Associate Professor Eng., Ph.D. University of Petroşani*
[2] *Associate Professor Eng., Ph.D. University of Petroşani*

1.1 The future of electrical energy

The electrical energy demand is increasing in the developed economies. Some aspects determine major structural changes as well as of electrical demand as the offers with important impact above electrical energy management:

- deindustrialization process of these economies;
- the present and future risks of environmental changes;
- the mixed energetically fuel changes;
- the growth of beneficiary aware regarding energy using.

The important energy customers and even the new power suppliers were established centralized as location, power and demand/supply power which were afforded in analyze of functional electrical transport system (RET). The national electrical transport structure has led taking into account technical and economic criteria as well as the safety applied to supply, transport and distribution system [5].

Regarding the European Parliament of the Council Directive 2010, each country has to control the own production/consume balance in case of necessary safety level achievement between different systems.

1.2 Energy from renewable sources

It is essential for approaching the climate changes to recognize the high level of various types of energetically sources as well fossil as renewable sources into a rational mode, sustainable and efficient as cost parameter. It is well known that the efficient input of energy from renewable sources vary in dependence with development level for each country or region [2].

The energy costs from renewable sources are increasing with the growth of technology development. However, some types of renewable sources energy could be expensive than some conventional sources addicting a supplementary costs above user. Some measurements for stability of transport system include: the develop of electrical energy structure, extending of interregional operation structure; the management of demanded stock when a higher intermittent energy of renewable sources are introduced.

1.3. The mixed sources of electrical energy

Both the coal fossil energy production and nuclear energy are playing an important role in energetically system through energy supply at base of load curve ant through the positive contribution at the feed with fossil fuel because the coal and uranium reserves are spread more than another fuel like petroleum and natural gases.

The thermal power plants have also an important role due to pliable of reserve capacity and the nuclear energy offers an important advantage in supply energy without emissions [4].

The energy based on coal will remain the major factor for the load curve submissive of the acute laws viewing the emission level for different nations and regions. The coal power plants have to embrace the policy of the Best Available Technology (BAT) and a clean technology based on coal as Integrate Gases Coal Cycle (IGCC) and technologies as Advanced Ultra Super Critical (A-USC).

The safety is more important priority for nuclear energy.

2. THE DOUBTFULNESS AND MAINTENANCE OF RET

The important elements which assure the safety and certain electrical supply are including the interconnection capacities and electrical dissipated engender. The political measurements should promote the innovation in technology, devices, services and business examples for assure a high certain of supplying.

These could provoke the research, demonstrations and develop activities to continue the innovation for all technologies with low carbon emissions pertinent for a new energetic system and also technologies for caption and stock the carbon, technologies for electrical energy stocks, updating technologies for distribution system, technologies for intelligent electrical measurements as well as renewable sources and electrical efficiency.

It is obviously that the renewable sources will affect the individual system operation into a significant way and their doubtful prediction is contributing to the base of unplanning transitory flows. Develop of U.E involves a conversion for energy using mode and the energy sources as well as the transport and distribution system function.

The responsibility of intelligent structures is consisting in assuring the safety, certain and sustainable economic function of electrical energy both the conventional power plants and distributed sources from customers. Also it is necessary to raise the efficiency of energetically process viewing the environmental safety, cost diminishing and services quality.

The scope of planning the transport structure is to assure a coordinating develop for a durable, efficient and economical transport system in benefit of customers on the long period of time. The main criterion in transport system is the completeness of energetically system and holding out for a several pre-established contingencies.

Some doubtfulness could appear:

- the prediction in establish for new supplying power capacities, the installing data in dependence with the price incertitude on the electrical market;
- the prediction for new capacities emplacement and their controller mode;
- the prediction of decommission of existing supply capacities;
- the supply costs and prices;
- the energy production prediction;

The incertitude of consume prediction grade is lowest with the other incertitude as raise and annual variation. The market is international and the changes

between interconnections will depend by difference of the electrical energy price in the interconnected systems.

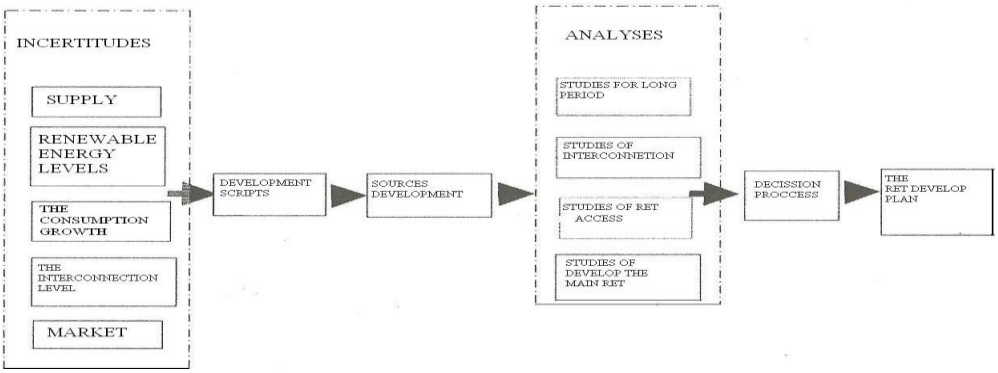

Fig.1. The doubtfulness in process of planning the transport structure

3. CONCLUSIONS

The important aspects of interconnections are: the conversion of transport interconnection rates and then in the intern system as a result of reactions at the price signal; the necessity of international coordinator planning; the assuring of financial support for new interconnections and financial support for intern system.

It is necessary to emphasis the raising number of uncontrolled plants but which demand also power for system services of controlled plants and for interconnection. This category is based on eolian power plants as 300-1800 MW power. The average power of turbine is about 30% from installed power. The higher power in eolian power plants involves a lot of number of interconnection capacities with proximity systems, a market with adjustable electrical power, the increasing of control and reactive power sources.

REFERENCES

[1]. Leca A., et al., *Managementul energiei,* Agir Publishing House, Bucharest, 2007

[2]. The 2015 International Electricity Summit, Okinawa, 2015

[3]. www.europa.eu/rapid/search ResultAction.do

[4]. www.eurelectric.com

[5]. Popescu A., et al.,. *Planificarea dezvoltarii sistemului energetic national in actualele conditii ale pietei de energie electrica*

[6]. Stochitoiu M., Gruber A.C., *The electric power plant impact reduction above the environment*, SIMPRO, Petrosani, 2013

Annals of the University of Petrosani, Electrical Engineering, 17 (2015)

RESEARCHES REGARDING INCREASING RELIABILITY FOR AG-63 COMMAND BOXES USED IN FLAMMABLE MINES

DRAGOŞ FOTĂU[1], SORIN BURIAN[2], MIHAI MAGYARI[3], LUCIAN MOLDOVAN[4], MARCEL RAD[5], COSMIN COLDA[6]

Abstract: The paper brings forward the mechanical malfunctions, due to corrosion, occurred on AG-63 command boxes which are used in the flammable mines of Jiu Valley. Following the assessment of the command boxes, a series of mechanical malfunctions have been highlighted, such as: local and remote button command malfunction; malfunction of the screws of the terminal boxes and those of the inserters; malfunction of the door command levers and of their locking bolts. In conclusion in order to increase the reliability and maintenance level of the command box, and consequently the operational safety of the construction of the box, it is therefore required to reconsider the maintenance policy regarding the mechanical part of the box.

Keywords: reliability, command box, maintenance, malfunction.

1. INTRODUCTION

According to a traditional approach, the quality notion of a product involves the consideration of a category of characteristics such as the reliability, maintainability and availability, elements which impose a series of conditions for the operational safety of a product, and which lay the foundation of the quality of the service the product offers to its users [2].

[1] *D.Eng., Ph.D Candidate, scientific researcher, INDC-INSEMEX Petroşani*
[2] *Ph. D.Eng., scientific researcher II, INDC-INSEMEX Petroşani*
[3] *Ph. D.Eng., scientific researcher II, INDC-INSEMEX Petroşani*
[4] *Ph. D.Eng., scientific researcher III, INDC-INSEMEX Petroşani*
[5] *D.Eng., Ph.D Candidate, scientific researcher, INDC-INSEMEX Petroşani*
[6] *Ph. D.Eng., scientific researcher III, INDC-INSEMEX Petroşani*

One of the mostly met equipments in the underground flammable mines of Jiu Valley, used for the command and protection of conveyor belts' engines, is the AG-63 command box manufactured by SC Gr. Ind. Ecb SA [2]

Therefore, the researches regarding the estimation of its reliability indicators were carried out using the AG-63 command boxes installed in the Lonea underground mine.

2. THE ASSESSMENT OF MECHANICAL DEFECTS AND THE ESTABLISHMENT OF A DATA BASE AND OF THE EMPIRIC FUNCTION FOR THE DISTRIBUTION OF OPERATIONAL TIMES UNTIL A MALFUNCTION OCCURS

2.1. Mechanical defects analysis for the estimation of the indicators of reliability

The observation of the operation of the command boxes has highlighted the following mechanical defects [2]:

- The malfunction of local and remote command buttons;
- The blocking of bolts from the lids of junction boxes and bolts from cable entries
- The malfunction of doors command levers and their locking mechanisms;
- The occurrence of rust on the closing surfaces between the lid and the encasing of the command box;
- The occurrence of rust on the bolts which connect the encasing to the ground.

2.2. The establishment of the data base and of the empiric function of the periods of operation until the occurrence of a malfunction

The data base resulted from the daily reports of the electrical-mechanical department of Lonea mine was used to establish the moments when mechanical malfunctions occur on AG-63 command boxes. The period in which the operation of the AG-63 command boxes was observed occurred between January 2014 and July 2015, namely on a period of 18 months (1.5 years), on a lot (sample) of 21 AG-63 command boxes [1].

The line, ordered from the smallest value to the largest one, composed of n = 97 values resulted from the analysis and interpretation of the data base, line dealing with the times of operation of the command boxes until a malfunction occurs, t_i, in *hours*, for all 21 command boxes, for the entire period of 1.5 years: 880; 960; 1000; 1056; 1100; 1100; 1100; 1140; 1140; 1146; 1210; 1250; 1270; 1320; 1400; 1430; 1430; 1460; 1500; 1600; 1650; 1690; 1700; 1700; 1710; 1720; 1740; 1760; 1760; 1760; 1780; 1780; 1800; 1840; 1840; 1840; 1840; 1850; 1880; 1880; 1890; 1900; 1900; 1900; 1900; 1920; 1920; 1960; 1960; 1960; 1970; 1980; 2000; 2000; 2000; 2000; 2000; 2000; 2060; 2060; 2100; 2100; 2100; 2100; 2100; 2100; 2100; 2100; 2100; 2100; 2100; 2100; 2110; 2110; 2120; 2120; 2140; 2140; 2160; 2200;

2200; 2200; 2210; 2300; 2300; 2300; 2300; 2320; 2320; 2380; 2400; 2400; 2410; 2460; 2700; 2700 [1].

This line represents therefore a statistical S2 series where some of the values are repeated (the series is not composed of disjunction values). After having been processed it results the new line composed of n_1 = 50 distinct values, with different occurrence frequencies for each value.

The following relation is used to determine the empiric function of repartition of the time of operation:

$$\hat{F}(t) = \sum_{j=1}^{i-1} f_j \text{ , for } t_{i-1} \le t \le t_i,\ i = 2, 3, \ldots, 50. \quad (1)$$

3. THE ESTIMATION OF THE RELIABILITY PARAMETERS

The estimation of the reliability parameters for each metallic construction of the AG-63 command box is realised using the theoretic distribution laws, the calculus methods for all their parameters for each step as well as the test of accordance between the theoretic and the empiric functions [1].

The determinations were carried out using the Excel and MathCAD software, which are used for tables' calculations, respectively for graphic representations of the followed parameters [3].

Table 1: *The reliability functions which characterise the mechanical part of the command box and their comparison*

Theoretical distribution	The reliability function, R(t)	The maximum deviation, D_{max}	Risk, α	Critical value, $D_{\alpha,50}$	Validation
Exponential	$e^{-5,2\cdot10^{-4}t}$	0.448862	0.005	0.240387	No
Normal	$\frac{1}{2} - \Phi\left(\frac{t-1872,082}{397,161}\right)$ *or* $1 - \frac{1}{397,161}\frac{1}{\sqrt{2\pi}}\int_0^t e^{-\frac{1}{2}\left(\frac{x-1872,082}{397,161}\right)^2} dx$	0.137912	0.20	0.148389	Yes
Weibull binomial, Wp	$e^{-\left(\frac{t}{2060,404}\right)^{5,007}}$	0.117511	0.20	0.148389	Yes
Weibull trinomial, Wm	$e^{-\left(\frac{t-1,92\cdot10^{-6}}{2029,148}\right)^{5,437}}$	**0.114349**	0.20	0.148389	Yes

Four types of distributions were used in order to estimate the reliability parameters: namely the normal distribution, the Weibull binomial distribution, the Weibull trinomial distribution and respectively the exponential distributions, only the first three having been validated. The validation or non-validation of the reliability function was carried out taking into account the maximum deviation (which should be smaller than 0.3) using the method of the smallest squares [1].

With the help of the determined parameters of the three validated distributions, as well as for the non-validated exponential distribution, the main quantity indicators which characterise the reliability of each mechanical part of the AG-63 command box were determined and graphically represented.

The graphic representations of Figures 1, 2, 3 and 4 deal with the variation curves depending on the period of time, the main reliability indicators which characterises the mechanical part of the command box [1].

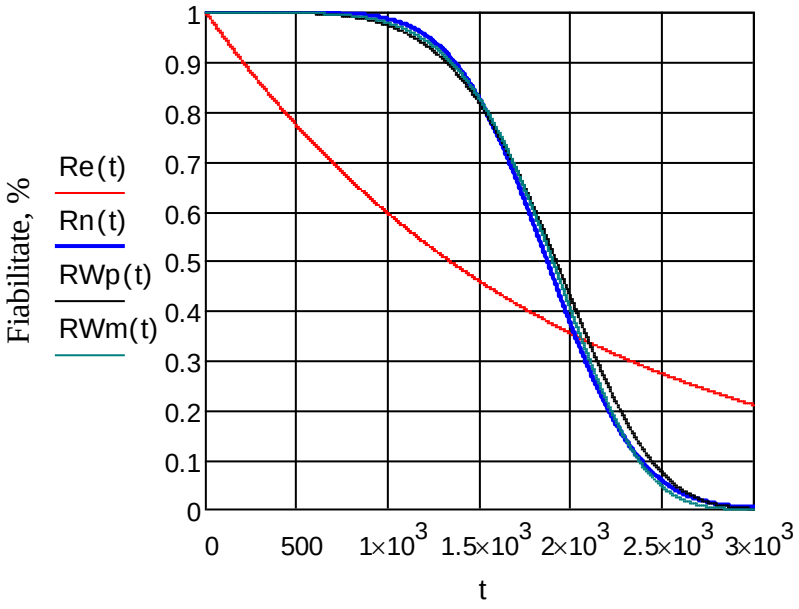

Fig. 1 The variation curves of the reliability functions
Re(t) – exponential; Rn(t) – normal;
RWp(t) – Weibull binomial; RWm(t) – Weibull trinomial

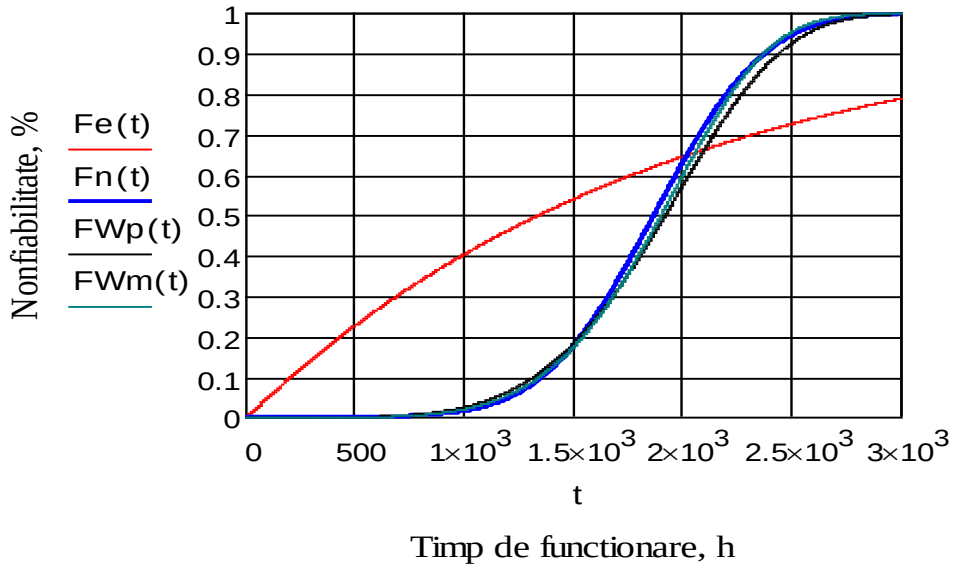

Fig. 2 The variation curves of the non-reliability functions
Fe(t) – exponential; Fn(t) – normal;
FWp(t) – Weibull binomial; FWm(t) – Weibull trinomial

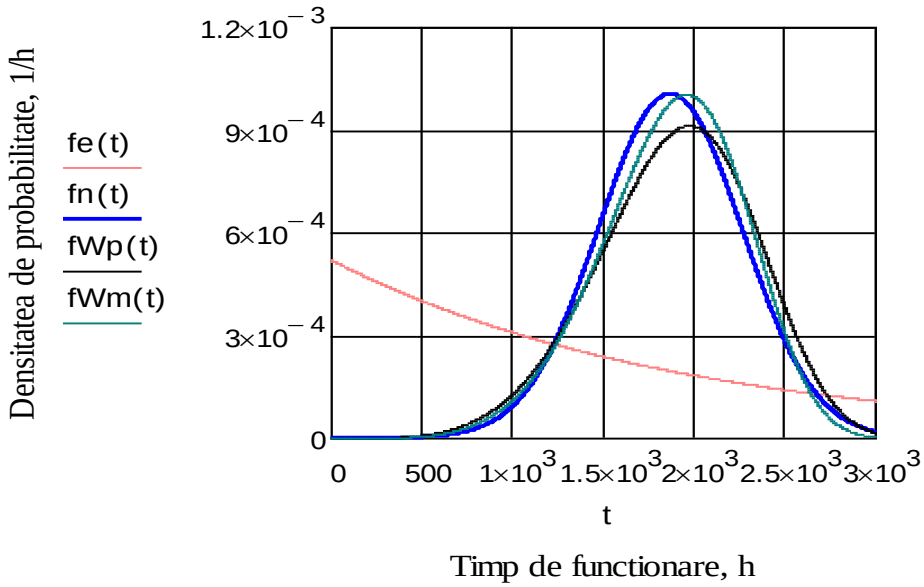

Fig. 3 The variation curves of the density of the probability of operational time
fe(t) – exponential; fn(t) – normal;
fWp(t) – Weibull binomial; fWm(t) – Weibull trinomial

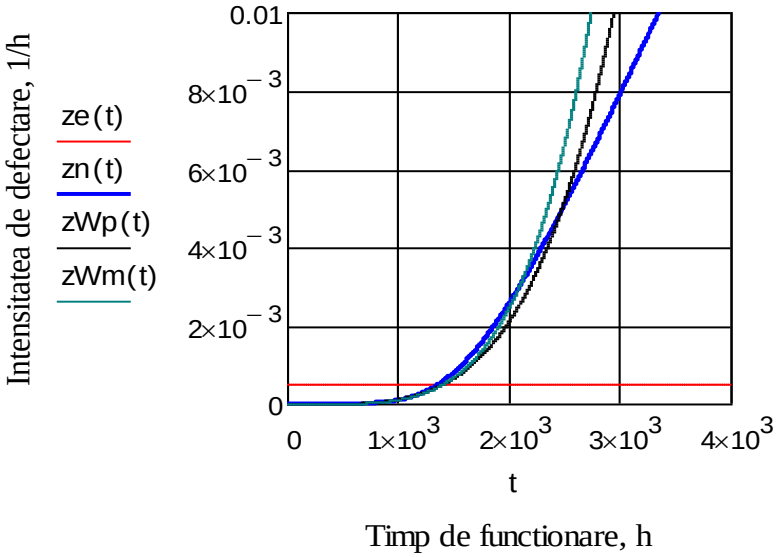

Fig. 4 The variation curves of the intensity or rate of malfunctions
ze(t) – exponential; zn(t) – normal;
zWp(t) – Weibull binomial; zWm(t) – Weibull trinomial

4. INTERPRETATION AND USE OF RESULTS

It results therefore the grouping tendency, as well as the overlapping one of the curves of reliability and non-reliability for the normal and Weibull distribution laws, from Figures 1 and 2, confirming the close values of the maximum distances between the empiric distribution (i.e. the experimental one) and that of the theoretical distributions. Moreover, it is confirmed that these distributions express with enough precision the most important reliability indicators.

Starting from the fact that according to the norms in force the preventive maintenance activity for the AG-63 command box is carried out underground, in 6 months of operation, i.e. 6 months × 30 days/month × 24 hours/day = 4320 effective *hours* of operation, allows the interpretation of the variation curves of the determined indicators. It is therefore considered the 6 months being a period of effective operation as the command box is continuously found inside a mine which adds to its corrosion.

If an 80% level of reliability is imposed, value which is quite good, and which is imposed for underground conditions in black coal mines, in order to ensure protection, it results in a flawless operational time of t_{80} = 1500 *hours*, which is transposed in calendar days in two months, meaning therefore that it should be expected, with an 80% probability (the risk being 20%), that during a 2 months' time no mechanical malfunction should appear at the AG-63 command box. It is a relatively small value compared to the six months period which is required for the technical inspection [1].

The probability for malfunctions to appear due to corrosion is practically zero for an operation of up to 1000 *hours* (i.e. 1.4 months), and respectively 60% for a period of 2000 *hours* (2.8 *months*). It is quite certain that the product does no longer meet the operating conditions regarding the mechanical malfunctions if the above value is exceeded. The values observed are way below the six months period foreseen for maintenance activities.

This variation of the reliability and non-reliability functions highlight the fact that once corrosion occurs, after roughly 1000 *hours* of operation, the phenomenon propagates quickly in time, fact which is also highlighted by the steep slope of the middle part roughly linear of the functions. It also brings forward the fact that the speed of corrosion is increased, or, the malfunction speed in general is increased.

The large malfunction speed, measured as *malfunction/hour* is best highlighted by the density curves of probability of the operation time from figure 3 and intensity or rate of malfunction in figure 4.

Analysing the variation in time of the intensity or the rate of malfunction it is therefore observed that for a period of operation of up to 1000 *h*, its value is practically zero, after which it is observed to get a strong increasing tendency which asymptotically tends to reach t = 3000 *ore* [1].

5. CONCLUSIONS

The reliability analysis carried out on the metallic construction of the AG-62 command box leads to the following conclusions:

- The breakdown of the metallic construction of the command box due to corrosion, which is the mathematic model expressed with the help of the normal and the Weibull distributions, and which is in perfect accordance with the previsions of the studied speciality literature;
- Considering the period established by the norms regarding the moment in which preventive maintenance activities are carried out, the reliability of the metallic construction is decreased resulting in an 80% reliability, which is absolutely necessary for the special conditions of underground black coal mining, for a period of only 1500 *hours* of operation, an equivalent of two months of continuous operation*;*
- In order to increase the level of maintainability and reliability of the command box and implicitly its operational safety of the actual construction of the command box, it is required to reconsider the design and the manufacture technology of the metallic part of the command box as to increase the resistance to corrosion of the functional parts, especially the contact surfaces between the casing and the lid, which mainly ensure the operational safety of the command box. Therefore, the materials used, the manufacturing technology of the contact surfaces need to be reconsidered, including the possibility to use metallic covers in order to obtain superior characteristics contact surfaces;

- Moreover, in order to reach the same target, it is required to reconsider the maintenance policy applied for the mechanical part of the command box, which can be realised through:
    - The improvement of the preventive and corrective maintenance activities which may lead to the avoidance of corrosion by thoroughly cleaning and protecting the functional surfaces;
    - The increase of preventive maintenance activities which may cover the characteristic periods of time resulted from the reliability assessment, which implies the change of the norms and regulations in force.

REFERENCES

[1] Fotău D., *Doctoral thesis: Researches regarding the increase of operational safety of electrical-mechanical equipments used in potentially explosive atmospheres* Petroşani 2016

[2] Fotău I., Rîşteiu M., Bălanescu I., *Trends in electrical power in mining,* Publishing house Sigma Plus, Deva, 1998

[3] Păsculescu V.M., Şuvar M.C., Vlasin N.I., Găman G.A., Florea D., *Computer modelling of flammable gas dispersion through leakages occurred in technological installations*, Proceedings of the15th International Multidisciplinary Scientific Geoconference SGEM 2015, Section Informatics, Geoinformatics and Remote Sensing, Volume I, pp. 77-84, Albena, Bulgaria, 2015.

Annals of the University of Petrosani, Electrical Engineering, 17 (2015)

VOLTAGE AND CURRENT HARMONICS SIMULATION

ILIE UŢU[1], MARIA DANIELA STOCHITOIU[2]

Abstract: Due to use of static power converters in modern controllable drives, one can notice the occurrence of disturbances in the mains, which entails voltage drops on the line, increase in loses, reactive energy consumption increase and interference with radio telecommunication systems. The real values of the current harmonics are different than the theoretically values, so we made some measurements of the current and voltage spectrum composition, in different winding working regimes. To this end we used a coprocessor for data acquisition in real time.

Keywords: voltage and current distortion, voltage spectrum composition, distorting running, width modulation, induction motor.

1. INTRODUCTION

To reinforce the conclusions regarding harmonic spectrum obtained from the theoretical point of view, we realized simulating static converter drive system - motor.

To achieve the numerical simulation of the electric drive we used MATLAB and Simulink software packages. For this purpose we designed a series of blocks of the type Simulink diagram for the different components of the drive units, which then interconnects to give the required final simulation schemes [1].

We started from mathematical equations describing the system operation, mathematical equations that we have systematized their functional blocks to implement software package Simulink.

The amplitude and order harmonic currents depend on the type rectifier (number of pulses and principle of operation), but the magnitude of harmonic currents depends on the angle control, α, of the power semiconductor elements [2].

[1] *Associate Professor Eng., Ph.D. University of Petrosani*
[2] *Associate Professor Eng., Ph.D. University of Petrosani*

2. SIMULATION DRIVE SYSTEM RECTIFIER - D.C. MOTOR

We made the comparison harmonic spectrum depending on the angle of the rectifier control for three - phase bridge rectifier completely ordered, which is most common in electrical drives [4].

We realized simulate different angles of the drive to control rectifier ($\alpha = 0^0$, 30^0, 45^0, 60^0, 90^0, 135^0).

The analysis performed following values for harmonics

	Harmonics order				
α	***1***	***5***	***7***	***11***	***13***
0^0	8	1,6	0,95	0,3	0,25
30^0	8	2,08	0,63	0,36	0,21
45^0	8	2,37	0,42	0,39	0,12
60^0	8	2,78	0,26	0,4	0,08
90^0	8	2,93	0,12	0,41	0,06
135^0	8	2,41	0,42	0,28	0,12

We can give these conclusions:

- For a three-phase bridge rectifier most significant harmonic currents are the order 5, 7, 11 and 13.
- Harmonic currents amplitude decreases with increasing harmonic order.
- The amplitude of the order harmonics 5 and 11 increases with increasing angle control between 0^0 and 90^0, increasing the amplitude of the order 5 being pregnant.
- Amplitude harmonic order 7 and 13 decreases with increasing angle control between 0^0 and 90^0, this decrease but with a lower rate than the increase harmonic order 5 and 11.

3. SIMULATION OF THE OPERATING SYSTEM MADE UP OF A FREQUENCY CONVERTER AND AN INDIRECT INDUCTION MOTOR

The drives static frequency converter - induction motor introduce additional current and voltage harmonics.

3.1. Comparison of harmonic voltage and current frequency

These harmonics are due to the presence of both the inverter voltage, which due to operating principle, has an output voltage that varies in speed, but also because the rectifier, which supplies a voltage inverter that is not regulated [1], [4].

The inverter output voltage frequency influence distorting regime introduced by the static converter.

In fig.1. we present the simulation results for the output voltage of the inverter and its harmonic analysis, for the frequencies 40 and 50 Hz.

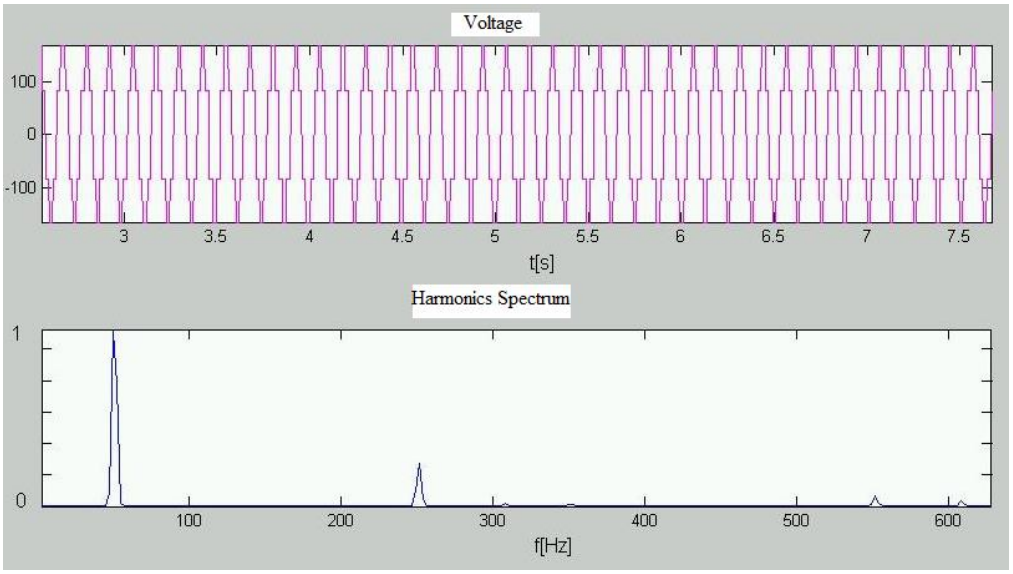

Fig.1. Voltage and harmonics spectrum for 50 Hz frequency

From these graphs is observed order harmonics 5, 6, 7, 11 and 12, harmonics that have significant value. Also it can be seen that the distorting regime increases with increasing frequency inverter output by increasing amplitude harmonic.

Figure 2 indicates the harmonic order 1 to 13 for the frequencies mentioned above.

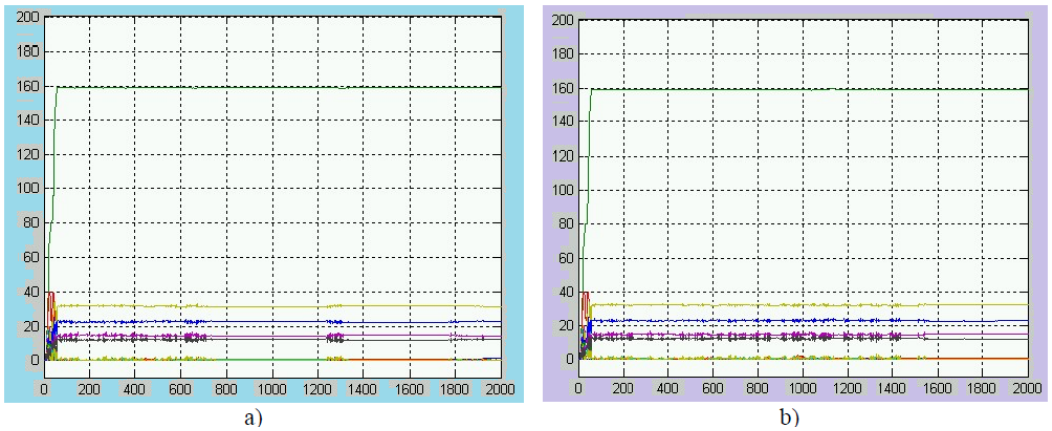

Fig.2. The voltage harmonics amplitudes for: a) 40 Hz, b) 50 Hz

The output current of the inverter is influenced by the frequency also, but distorting regime decreases with increasing frequency. Significant higher harmonics of the current have order 5, 7, 11 and 13 as can be seen from Fig. 3 - 4.

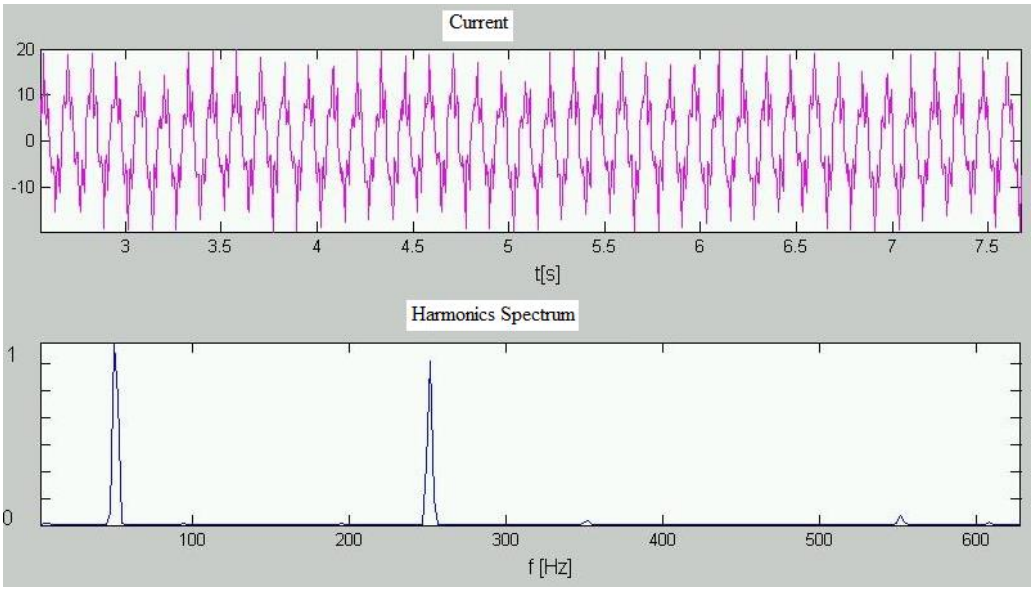

Fig.3. Current and harmonics spectrum for 50 Hz frequency

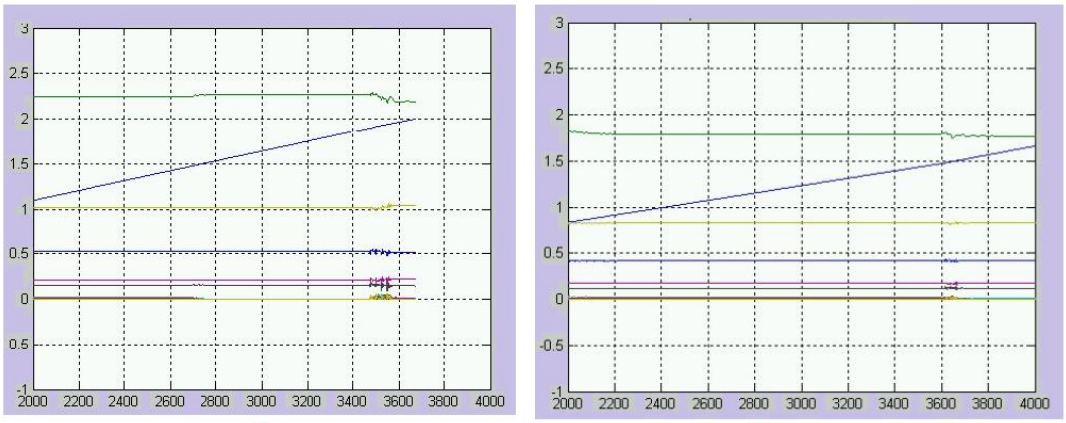

Fig.4. Amplitudes of harmonic current for: a) 40 Hz, b) 50 Hz

3.2. Harmonics voltage and current for a PWM inverter

The principle of PWM (width modulation) inverter brings significant improvements for distorting regime introduced by static frequency converters, especially at high switching frequencies [2], [3].

Figures 5 - 8 show the simulation results of a static frequency converter circuit by the DC inverter in its composition being an inverter width modulated (PWM inverter). Simulations were conducted for a carrier frequency 1000 Hz.

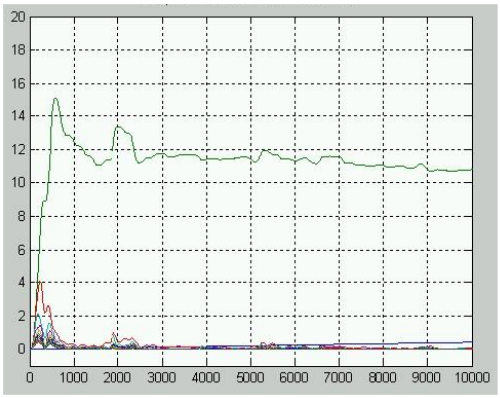

Fig.5. The variation of voltage harmonic amplitudes

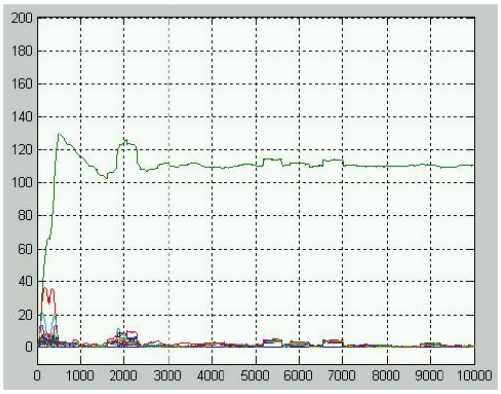

Fig.6. The vriation of currents harmonic amplitudes

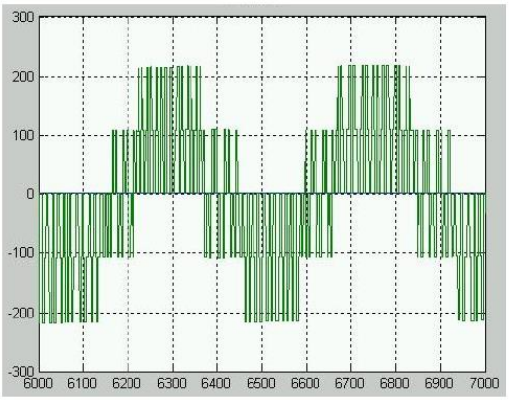

Fig.7. The waveform of the voltage for 50 Hz frequency

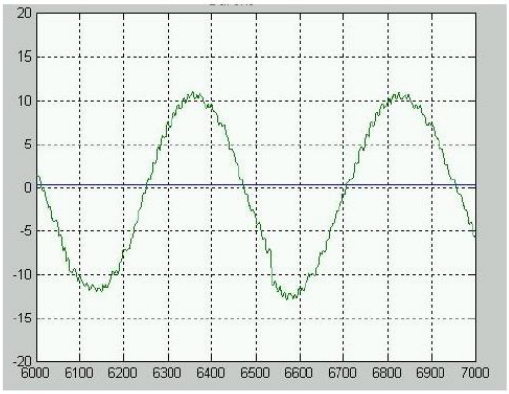

Fig.8. The waveform of the load current for 50 Hz frequency

4. CASE STUDY

We conducted laboratory measurements for the study distorting regime introduced drives static frequency converter-motors. The measurements were made for a 3 kW asynchronous motor powered at 380 V [1], [2].

4.1. The measurement results in U / f = ct

The inverter used is recommended to operate the U/f = ct a carrier frequency of 2 kHz. The measurement results are given in fig.9 - 10.

Fig.9. The voltage, current and frequency variations

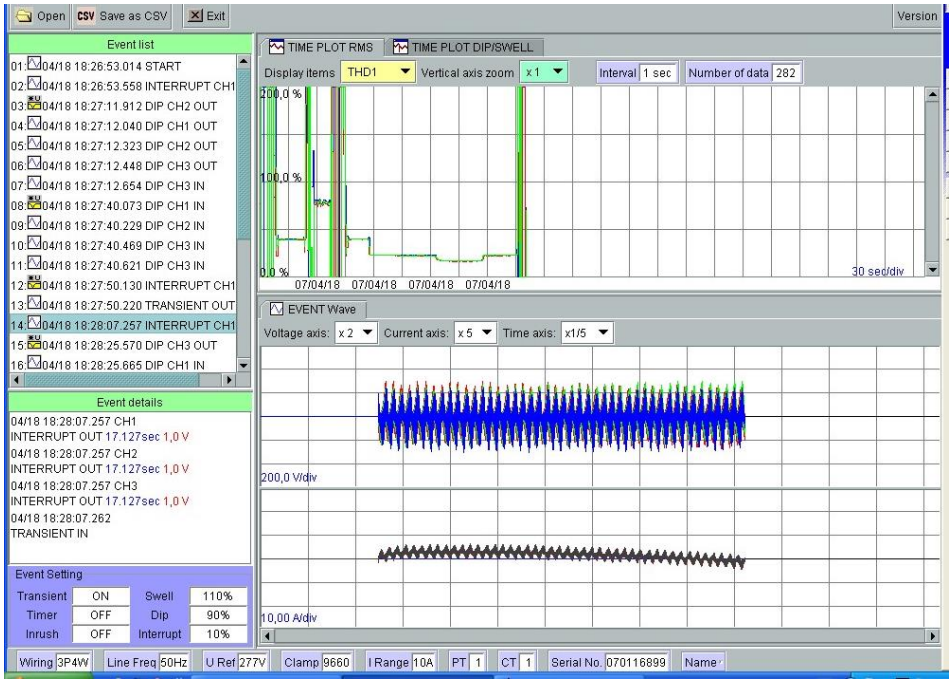

Fig.10. THD variation

4.2. The measurement results for vector control

Vector control inverter is used with a carrier frequency of 2 kHz. The measurement results are given in fig.11 - 12.

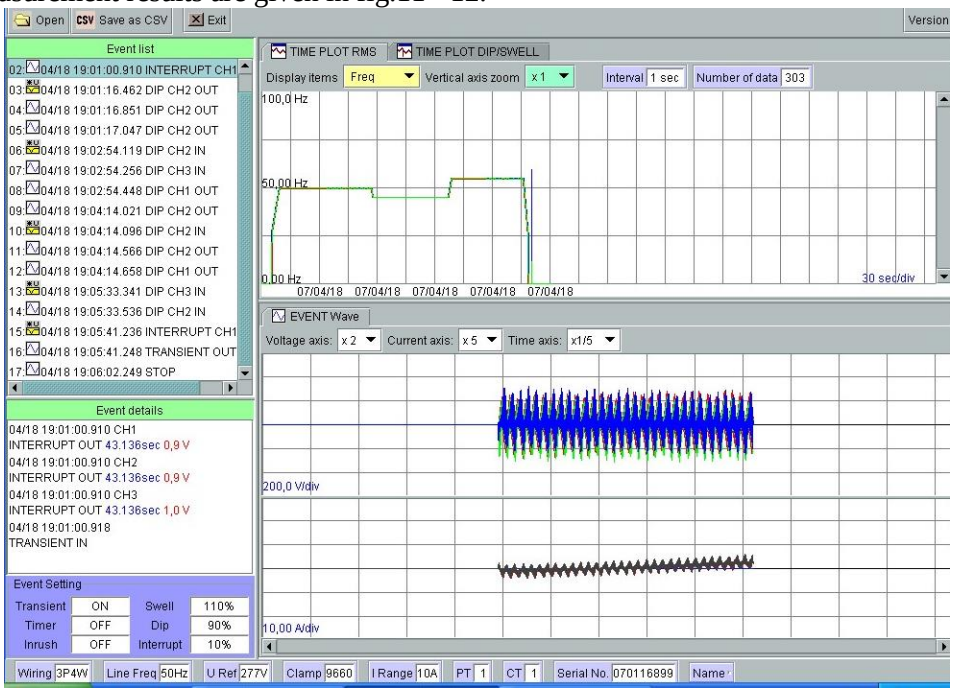

Fig.11. The voltage, current and frequency variations

The measurements were carried out at start-up, and changing the frequency and voltage at different values of load.

5. CONCLUSIONS

As seen from the results of measurements for U/f, distorting regime is stronger in case of voltage harmonics than the current ones. Once the frequency changing decreases the distorting regime so, at a frequency of 45 Hz we got THD = 22.9% (no load) and THD = 17.5% at full load and at a frequency of 55 Hz, THD = 22.4% (no load) and THD = 15.8% at full load.

In all cases, the distorted current regime is less than the voltage supplied to the induction motor. There harmonics of high order, who have powerful influences (eg harmonic order 40 which has an amplitude of about 30% of fundamental) harmonic influence due to high frequencies, controls the electric drive.

In the case of open-loop vector commands, distorting regime decreases with changing the frequency to 50 Hz value (carrier frequency is 2 kHz). It notes, however, keeping constant distorting regime at idle and under load.

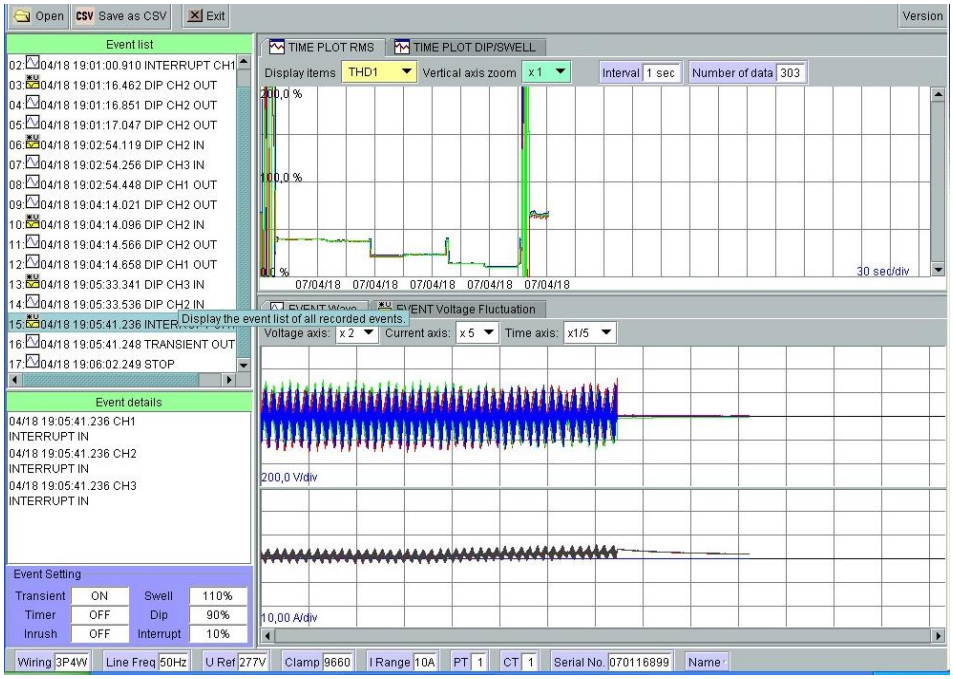

Fig.12. THD Variation

This was expected considering the advantages of vector control method that changes the value of the frequency and torque control loops independent task therefore not influence the distorting regime.

REFERENCES

[1]. Marcu M.D., Popescu F.G., Niculescu T., Pana L., Handra A.D., *Simulation of power active filter using instantaneous reactive power theory*. Harmonics and Quality of Power (ICHQP), IEEE 16th International Conference, Page(s):581 – 585, Bucharest, Romania, 25-28 May, 2014.

[2]. Marcu M.D., Popescu F.G., Samoila B. L., *Modeling and simuling power active filter using method of generalized reactive power theory*. Computer Science and Automation Engineering (CSAE), 201, IEEE International Conference.

[3]. Samoila B.L., Marcu M.D., Popescu F.G., *Equipment Designed to Control a Heating Hybrid System with Solid Fuel Boiler and Solar Panels*, Proceedings of the 7th International Conference on Renewable Energy Sources (RES '13), pag. 106-111, ISBN: 978-1-61804-175-3, Kuala Lumpur, Malaysia, April 2-4, 2013.

[4]. Uțu, I. *Reduce the Harmonics from Mining Extraction Plants operated with DC Motors.* Proceedings of the 12th International Conference on Instrumentation, Measurement, Circuits and Systems (IMCAS'13), Kuala Lumpur, Malaysia, 2013.

Annals of the University of Petrosani, Electrical Engineering, 17 (2015)

ANALYTICAL MODELING OF PROTECTION RELAYS

LEON PANĂ[1], FLORIN-GABRIEL POPESCU[2]

Abstract: A small part of power system, including one or more protection systems, is modeled by using mathematical techniques: Markov theory, renewal theory, Petri nets and Monte Carlo simulation. In this paper the Markov models from protection systems are discussed and analyzed.

Keywords: reliability, protection system, failure to operate, mal-trip, power system.

1. INTRODUCTION

An industrial supply network system consists of a combination of lines or cables, power transformers and incoming power sources including co generators. The power cables, overhead lines and transformer form the main supply network, which provides a reliable power transmission from sources to loads.

A protection system protects the power system from the harmful effect or faults. a fault is an abnormal system condition, which is in most cases a short circuit and occurs as a random event. In general, protection systems do not prevent damage to the power system, they operate after some detectable damage has already occurred.

In this section an overview of protection models used in reliability analysis and the stochastic models of the protection systems used in other area will be presented. The models are not discussed in full detail, only the main characteristics are presented. For more information, references are included.

Of the qualities required of the protection systems [1], [3], the two of main interest to us here are:

[1] *PhD. Lecturer, Eng., University of Petrosani*
[2] *PhD. Lecturer, Eng., University of Petrosani*

Selectivity or discrimination - The protection system is effectiveness in isolating only the faulty part of the system.

Stability - The property of remaining in operation with faults occurring outside the protected zone.

In other words, the power system protection should isolate the fault and refrain from action for the rest. These two aspects of the protection lead to two aspects of the reliability of the protection as defined by the IEC [1].

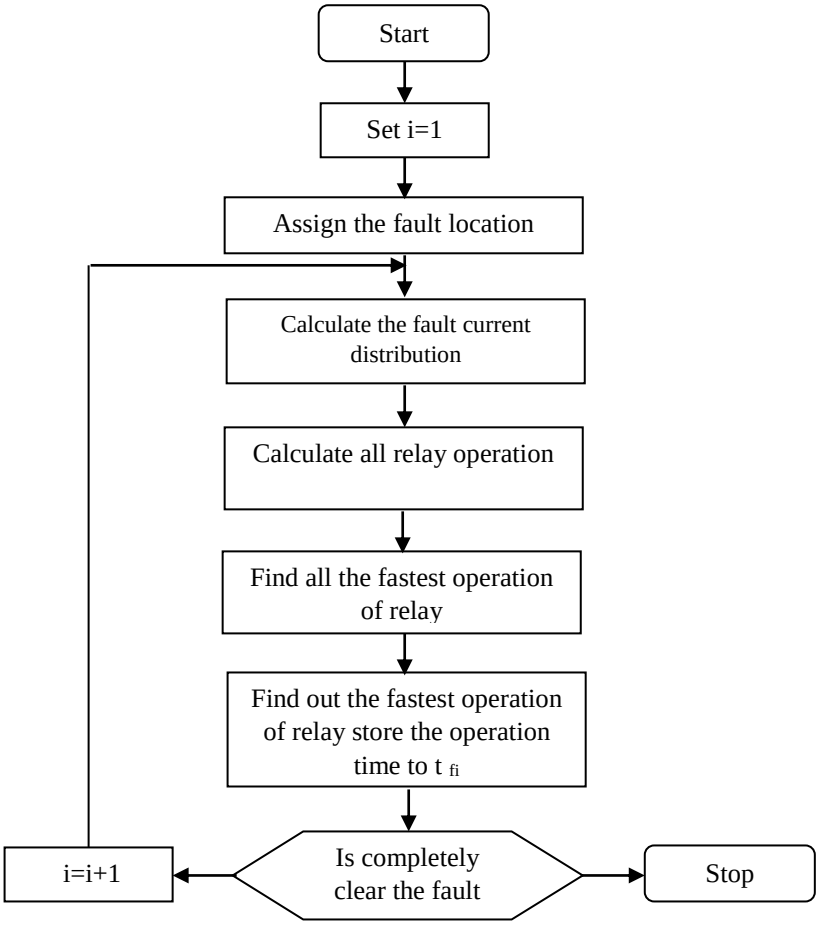

Fig. 1 The flow chart for the reliability algorithm to clear one simulated faults

Reliability of protection - The probability that a protection can perform a required function under given conditions for a given time interval.

Dependability - The probability for a protection of not heaving a failure to operate under given conditions for a given time interval.

Security - The probability for a protection of not having an unwanted operation under given conditions for a given time interval.

Reliability is generally defined as a measure of certainly that a piece of equipment or system will perform as installed.

In figure 1 is illustrated the flow chart for the reliability algorithm to clear one simulated faults.

Here the two principal failure modes of the protection appear, namely, failure to operate and unwanted operation. These two terms will reappear further on, but there is more to failure of the protection than this. For example, the unwanted operation can be spontaneous, or due to an event in the power system (often a fault outside the zone to be protected, i.e. an external fault). The failure can be due to a relay failure, a circuit breaker failure, a current transformer failure or even due to an error in the calculation of the setting. The first aspect of the protection to be modeled in a stochastic way was the fault clearance time [1], [2]. Once the probability density function of the fault clearance time is known, of the fault clearance time is known, the required time-grading can be calculated for any given value of the acceptable chance of unwanted operation. A similar concept is used for stochastic assessment of transient stability [1], [2], [3].

2. SYSTEM PROTECTION MODEL AND RELIABILITY ALGORITHM

At the occurrence of fault on a power system, the current is almost always greater then the pre-fault load current in the components in the vicinity of the fault. The operational time of an overcurrent relay depends on its operating characteristics.

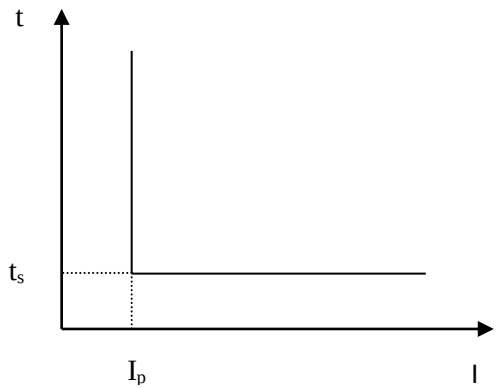

Fig. 2 Overcurrent relay with definite-time characteristic

Figure 2 shows the operational time of an overcurrent relay with definite-time characteristic. Such a relay does not operate (operating time is infinite) as long as the current magnitude is less than I_p. If the current magnitude exceeds I_p the relay operate after T_s seconds.

In order to design a protection system, one must be able to represent and evaluate the performance of protection systems. Thus, methods of representing the performance of relays alone and in relation to other relays of the protection system are required. In this section, the *relay-unit* that has the simplest operating characteristic is introduced. The operating characteristic of any relay can be represented by a set of relay-units. Moreover, this section presents a method for representing the performance of a protection system.

A relay-unit (denote by r) is the relay that has a simplest operating characteristic, as shown in figure 3. Such a relay operates after a pre-set delay times t_s, in case of any fault for which operating quantity q is above the pick-up value q_p.

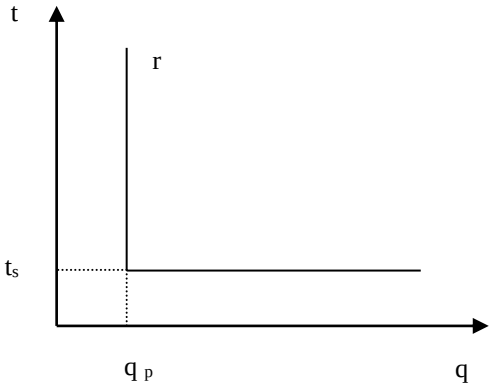

Fig. 3 Unit-relay is operating characteristic

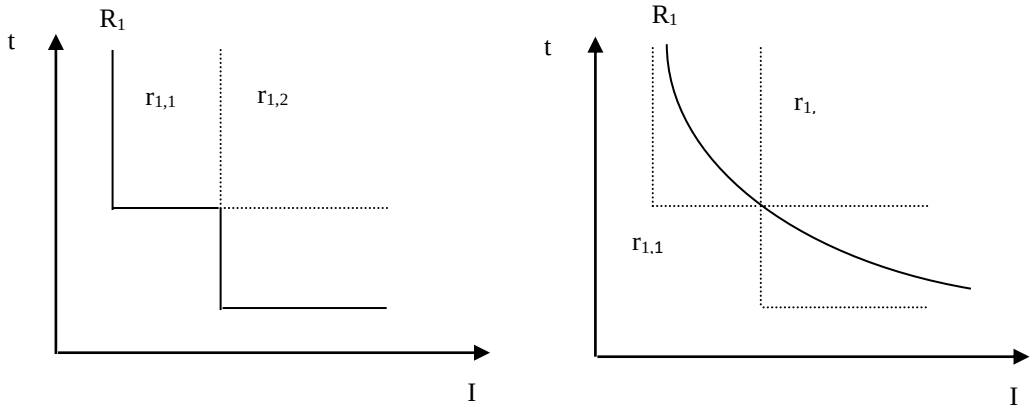

Fig. 4 Complex characteristics by combining relay-units

In general, the operating quantity of a relay-unit can be any function of the currents and voltages of the component being protected.

As overcurrent relay with a definite time characteristic is an example of a relay-unit with the component current at the operating quantity. Such a relay operates for all currents above the pick-up setting of the relay. It is possible to set up a relay-unit that operates for values smaller than the pick-up value and take no action for values above the pickup. Under-voltage and one step impedance or distance relays are examples of such a relay.

Due to simplicity of the operating characteristics of relay-units, every relay-operating characteristic can be represented by a combination of a set of relay-units.

In figure 4 two steps and an inverse characteristic are represented by a combination of two relay-units. In this paragraph, a small letter "r" denotes each relay-unit (e.g. r_1, r_2) and each protective relay that consist of one or more relay-units is denoted by a capital "R".

The dynamic equation for the OC relay operation time calculation is defined by IEEE standard C37.112-1996 as shown in equation (1):

$$\int_0^{T_0} \frac{1}{t(I)} = 1 \tag{1}$$

where:

t(I) Is the relay disc traveling time from 0 to operating distance at fault current I

For the three consecutive fault currents, I_1, I_2, I_3 the t_{actual} is calculated as follows:

$$\begin{aligned} &\int_0^{t_{f1}} \frac{1}{t_1} dt + \int_{t_{f1}}^{t_{f1}+t_{f2}} \frac{1}{t_2} dt + \int_{t_{f1}+t_{f2}}^{t_{actual}} \frac{1}{t_3} dt = 1 \\ &\frac{t_{f1}}{t_1} + \frac{t_{f2}}{t_2} + \frac{1}{t_3}\left(t_{actual} - t_{f1} - t_{f2}\right) = 1 \\ &t_{actual} = \sum_{1=1}^{2} t_{fi} + t_3\left(1 - \sum_{1=1}^{2} \frac{t_{fi}}{t_i}\right) \end{aligned} \tag{2}$$

where:

t_1, t_2, t_3 are the relay operating times at fault current I_1, I_2, I_3 respectively.

The inverse definite minimum time lag (IDMTL) over current relay (OC) operating time for "n" steps of fault currents with n consecutive fault currents is shown in following equation:

$$t_{actual} = \sum_{i=1}^{n-1} t_{fi} + t_n\left(1 - \sum_{i=1}^{n-1} \frac{t_{fi}}{t_i}\right) \tag{3}$$

The protection is here considered to consist of four parts:

- Main protection
- Backup protection
- Breaker failure protection
- Circuit breaker

A protection system has two alternative ways in which it can be unreliable it may fail to operate when it is expected to (referred to as *fail-to-trip*), or it may operate when it is not expected to (referred to as mal-trip). This leads to a two-pronged definition of the reliability of protection systems.

3. ASSUMPTION AND SITUATION DESCRIPTION

The following assumptions are used in modeling the system:

- After a failure to operate, which is followed by a repair, and after maintenance the relay is working properly.
- The times to failure of a relay (TTF) are independent and exponentially distributed with parameter p. This means that if a relay is last seen healthy at time t_h, than the chance the relay is dormant at time t is equal to:

$$P(T < t) = 1 - e^{-p\cdot(t-t_h)} \quad \text{for } t > t_h \tag{4}$$

  Here T is the moment at which the relay becomes dormant.
- Times between short circuits (TBSC) are independent and exponentially distributed with parameter λ. Since short circuits are cleared immediately in the model, the chance that a short circuit will happen in the next interval of time t is equal to:

$$P(T_{sh} < t) = 1 - e^{-\lambda\cdot t} \tag{5}$$

  Here T_{sh} denote the time to the next short circuit.
- The time between two successive maintenance (TBM) is independent and in a protection system with "n" relay, the TBM is exponentially distributed with parameter μ/n. All "n" relays are maintained at the same time. The average number of relays maintained in one unit of time then equalsμ.

Due to characteristics of matrix T, the changes in $P_i(t)$ will diminish in $t \to \infty$. With this, the set of differential equations reduces to set of linear equations having the form:

$$T \cdot P = O \tag{6}$$

where

P a column vector whose i^{th} term is steady-state probability of residing in state i

Since the elements in each columns of matrix A add up to zero, the determinant of T in zero and, therefore, the equations in (9) are not linearly independent.

Each equation is linear combinations of others. To provide an additional equation, the simple fact is recognized that the state probabilities must add up to 1 at time t, and therefore:

$$\sum_{k=1}^{n} P_k = 1 \tag{7}$$

For this reason, the steady-state probabilities can be obtained by solving the following matrix equation:

$$T' \cdot P = C \tag{8}$$

where:

- T' a matrix obtained from matrix A by replacing the elements of an arbitrarily selected row p by ones
- P a column vector whose i^{th} term is the probability of residing in state I
- C a column vector with the p^{th} element equal to one and other elements set to zero

In figure 5 the standard graphical representation of the Markov model is shown. The model contains two relays. Short circuit lead to the fail-to-trip if both relays are dormant at the time of occurrence at the short circuit. Maintenance is performed simultaneously at both relays. The times between maintenance are exponentially distributed with parameter $\frac{\mu}{2}$.

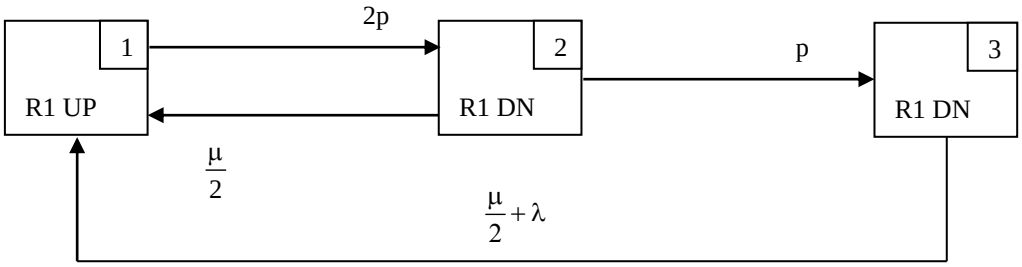

Fig. 5 State-space diagram for a system comprising two protective relays

The three states of this model are defined as follows:

State 1: In this state both relays are healthy. The short circuit and the maintenance do not cause a transition when the system is in this state. Both relays can fail with rate p. this cause a total transition rate out of state one, equal to 2p.

State 2: In this state one of the relays is dormant. In this case short circuits do not have any influence on the state of the model because the relay that is healthy will work properly. Maintenance with rate $\frac{\mu}{2}$ will cause a transition to state 1 while the failure of the healthy relay with rate p, will cause a transition to state 3.

State 3: In this state both relays are dormant. Maintenance with rate $\frac{\mu}{2}$ will cause a transition to state 1. Short circuits with rate λ, while the system is in a state 3 will cause a failure to operate and the repair of both relays that is represented by a transition to state 1.

The matrix T is:

$$T = \begin{pmatrix} T_{11} & T_{21} & T_{31} \\ T_{12} & T_{22} & T_{32} \\ T_{13} & T_{23} & T_{33} \end{pmatrix} = \begin{pmatrix} -2p & \frac{\mu}{2} & \frac{\mu}{2}+\lambda \\ 2p & -\frac{\mu}{2}-p & 0 \\ 0 & p & -\frac{\mu}{2}-\lambda \end{pmatrix} \tag{9}$$

The matrices T' and C is:

$$T' = \begin{pmatrix} -2p & \frac{\mu}{2} & \frac{\mu}{2}+\lambda \\ 2p & -\frac{\mu}{2}-p & 0 \\ 1 & 1 & 1 \end{pmatrix} \quad , \quad C = \begin{pmatrix} 0 \\ 0 \\ 1 \end{pmatrix} \tag{10}$$

Solving equation (8) results in:

$$P = T'^{-1} \cdot C = \begin{pmatrix} P_1 \\ P_2 \\ P_3 \end{pmatrix} = \frac{1}{12\lambda p + 8p^2 + 2\lambda\mu + 6p\mu + \mu^2} \begin{pmatrix} (2\lambda+\mu)(2p+\mu) \\ 4p(2\lambda+\mu) \\ 8p^2 \end{pmatrix} \tag{11}$$

4. CONCLUSION

The method is analytical.

Very general results can be obtained that are independent of the precise shape of the distribution function.

REFERENCES

[2]. Anderson P.M., *Reliability modeling of protective systems*, IEEE Transactions on Power Apparatus and Systems, vol.103 (1984), p.2207-2214.

[3]. Anderson P.M. and Agarwal S.K., *An improved model for protective systems reliability,* IEEE Transactions on Reliability, vol. 41 (1992), p. 422-426.

[4]. Anders G..J., *Probabilistic concepts in electric power systems*, New York: John Wiley & Sons, 1990.

Annals of the University of Petroşani, Mining Engineering, 17 (2015)

LABVIEW SIMULATIONS USED IN A.C. CIRCUITS BEHAVIOR STUDY

BRANA LILIANA SAMOILA[1], SUSANA LETITIA ARAD [2]

Abstract: The paper shows some of the LabView simulations we made for studying the a.c. circuits. These virtual instruments are used during the teaching and learning activities where they turned out to be very helpful for students aiming a better understanding of the electric circuit behavior under different conditions. We made them simple, easy to use and intuitive, being an alternative, more flexible, method of practice in the laboratories.

Keywords: virtual instrument, a.c. circuit, electrical engineering education

1. INTRODUCTION

LabVIEW is the acronym for Laboratory Virtual Instrument Engineering Workbench. Together with specific hardware devices, modern complex systems for data acquisition and processing can be developed. LabVIEW is a graphical programming environment that makes not necessary to know a programming language itself, using algorithms designed as a flowchart (diagram) instead of text instructions.

Programs developed in LabVIEW are called virtual instruments (VI) as they are like actual instruments [2].

Data entry can be provided in different ways: user input via keyboard or mouse; extracted from data files located on memory devices; received via video camera, network card, data acquisition system, etc.

Output data can be displayed on the screen or may be saved in data files so that these will then be accessed by the user or by other programs.

.

[1] *Associate Professor, Eng., PhD, University of Petrosani, Romania*
[2] *Professor, Eng., PhD, University of Petrosani, Romania*

2. VIRTUAL INSTRUMENT FOR SIMULATING AN R-L-C SERIES A. C. CIRCUIT

The simulated circuit is shown in Fig. 1.

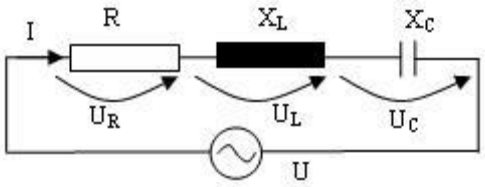

Fig. 1 A. C. series R-L-C simulated circuit

The impedance, Z, of a component or a circuit is defined [1], [7] as:

$$\underline{Z} = R + jX \tag{1}$$

where R is the resistance, j is the imaginary unit, and X is the reactance.

Capacitors and inductors are both components which can store energy: capacitors store it in an electric field and inductors in a magnetic field. Ideal capacitors and inductors are assumed to have zero resistance and so we have pure imaginary impedance (reactance).

$$X_L = \omega L; \quad X_C = \frac{1}{\omega C} \tag{2}$$

$$X = X_L - X_C \tag{3}$$

The total impedance in a RLC series circuit is given by:

$$Z = \sqrt{R^2 + (X_L - X_C)^2} \tag{4}$$

When speaking about the phase difference, it can be calculated as:

$$\varphi = arctg\frac{X}{R} = \arccos\frac{R}{Z} \tag{5}$$

The current RMS value is:

$$I = \frac{U}{Z} \tag{6}$$

The voltage U is:

$$\underline{U} = \underline{U}_R + \underline{U}_L + \underline{U}_C \tag{7}$$

All these values are given in the virtual instrument, whose front panel is presented in Fig. 2 [6].

Virtual voltmeters indicate the RMS voltages across the three ideal elements: resistor, inductor and capacitor and the ammeter measures the current [3], [5]. A gauge type control gives the phase difference between the current and the total voltage.

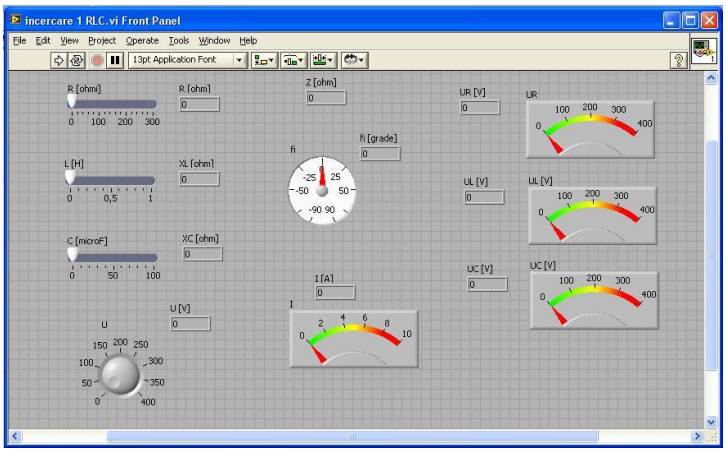

Fig. 2 Front panel of RLC series circuit VI

There is a minimum value of the series impedance, when the voltages across capacitor and inductor are equal and opposite.

$U_L = U_C$

In an RLC series circuit in which the inductor has no internal resistance it is possible to have a large voltage across the inductor, an equally large voltage across capacitor but, as the two are 180° degrees out of phase, their voltages cancel, giving a total series voltage that is equal to U_R.

At resonance, the voltages across the capacitor and the pure inductance cancel out, so the series impedance takes its minimum value: $Z_o = R$. Thus, if we keep the voltage constant, the current is a maximum at resonance.

Such a resonance situation is represented in Fig. 3.

3. VIRTUAL INSTRUMENT FOR SIMULATING AN R-L-C PARALLEL A. C. CIRCUIT

The simulated circuit is shown in Fig. 4.

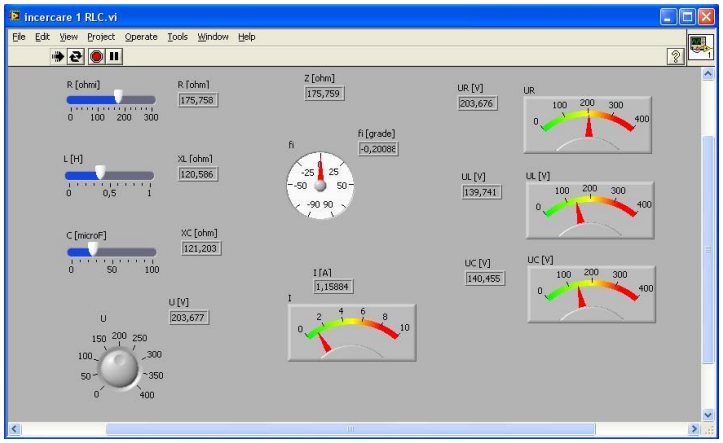

Fig. 3 Series resonance

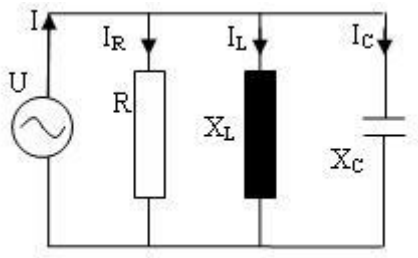

Fig. 4 RLC parallel simulated circuit

With Kirchhoff's first theorem, [1], [7] we can write:

$$\underline{I} = \underline{I}_r + \underline{I}_L + \underline{I}_C \tag{8}$$

$$I^2 = I_R^2 + (I_L - I_C)^2 \text{ or } I^2 = \frac{U^2}{R^2} + \left(\frac{U}{X_L} - \frac{U}{X_C}\right)^2 \tag{9}$$

From (13) it results:

$$\frac{I}{U} = \sqrt{\frac{1}{R^2} + \left(\frac{1}{X_L} - \frac{1}{X_C}\right)^2} = \frac{1}{Z} \tag{10}$$

The amount 1/Z is called admittance and it is noted with Y. Its components are the conductance G and the susceptance B.

$$\underline{Y} = G - jB \tag{11}$$

The front panel of the VI which may be used to study a RLC parallel circuit is presented in Figure 5 [4].

A parallel circuit containing a resistance, R, an inductance, L, and a capacitance, C, produces a parallel resonance **(**also called anti-resonance) when the resultant current through the parallel combination is in phase with the supply voltage. At resonance there will be a large circulating current between the inductor and the capacitor due to the energy of the oscillations. So, parallel circuits produce current resonance (fig. 6) [1], [3], [6].

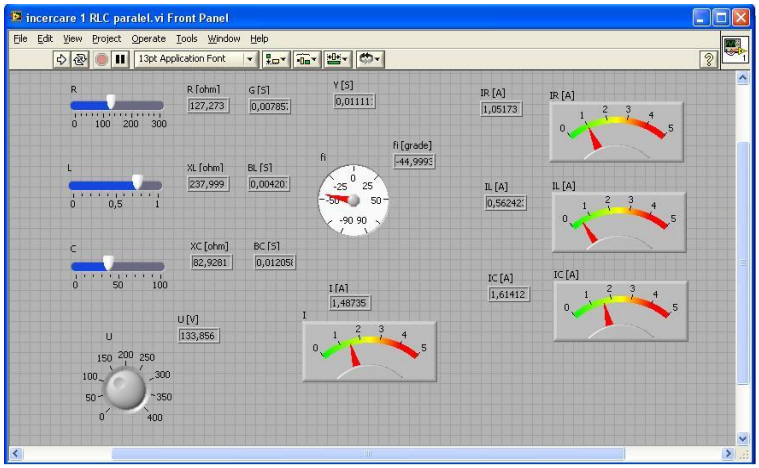

Fig. 5 Front panel of a RLC parallel circuit

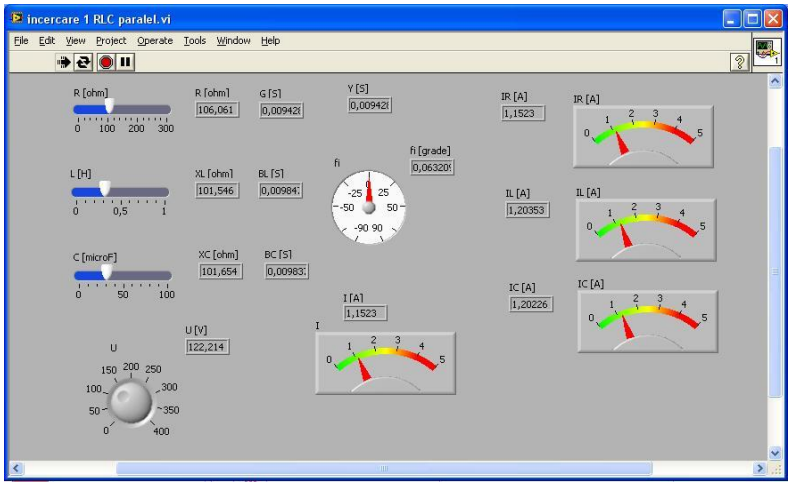

Fig. 6 Parallel resonance

4. CONCLUSIONS

In this paper we have presented two of the virtual instruments we achieved to study the direct current and the alternating current circuits. They proved to be very helpful during the teaching activities. They are simple, easy to use, flexible, allowing an intuitive laboratory practice. At the laboratory activities, the students are able to easily build circuits, to put into practice the theoretical knowledge and experience safely.

Beside the virtual instruments presented in this paper, we made more VI-s in order to study Ohm's law, calculation of equivalent resistance of resistors connected in series or parallel, resistance measuring methods such as: Wheatstone bridge, substitution method, comparison method, voltmeter and ammeter method, study of power distribution in RLC a.c. circuits etc.

All virtual instruments can be used as sub-VI-s in more complex applications.

REFERENCES

[1] Arad L. S., *Electrotehnica,* Didactic and Pedagogic Publishing House, Bucharest, 2004.

[2] Patrascoiu N., *Achizitie de date. Instrumentaţie virtuala*, Didactic and Pedagogic Publishing House, Bucharest, 2004

[3] Pop M., *Masurari electrice*, Universitas Publishing House Petrosani, 2010

[4] Samoila L., Arad S., Utu I., *Virtual Instrumentation to Study D.C. and A.C. Circuits,* SATEE, Alba Iulia, 2014

[5] Uţu I., Marcu M., *Tehnici de masurare. Teorie si aplicatii.* Universitas Publishing House Petrosani,, 2004

[6] Utu I., Samoila L., *Masurarea marimilor electrice*, Universitas Publishing

[7] Uţu I., Marcu M., Orban M. D., *Electrotehnica,* University of Petrosani, 2001

Annals of the University of Petroşani, Electrical Engineering, 17 (2015)

DETERMINATION OF DISTRIBUTION NETWORKS SECTION BASED ON THE MINIMUM VOLUME OF CONDUCTION MATERIAL

DRAGOŞ PĂSCULESCU[1], SUSANA ARAD[2], VLAD MIHAI PĂSCULESCU[3]

Abstract: Besides a series of technical conditions, choosing conductors has to satisfy an economical criterion, namely to ensure the minimum cost value of electricity. This paper deals with the establishment of the optimum section based on the minimum volume of conduction material.

Keywords: conduction material, distribution network, minimum volume, section.

1. INTRODUCTION

For proper technical operation and financially profitability, conductors from electrical networks have to simultaneously fulfil a series of conditions which may be used as dimensioning of verification criteria. In case of networks supplied at one end and which have concentrated loads, currents from different segments have particular values [7].

In this regard, constructing a network with constant section of conductors in all segments is not financially rational. Especially when the lengths of the segments are high, and their load is very different, there may be obtained significant conduction material economies, by decreasing the section of conductors once with the decrease of currents from the segments towards the end of the network [4].

By generally adopting different sections in each segment, there is generated an issue for determining the number of unknowns equal to the one of the segments, for this purpose being needed to create an equation system of the same number.

[1] *Lecturer, Ph.D. University of Petrosani*
[2] *Professor, Ph.D. University of Petrosani*
[3] *Senior Researcher III, Ph.D. INCD INSEMEX Petrosani*

2. DISTRIBUTION NETWORKS' SECTION CALCULATION BASED ON THE MINIMUM VOLUME OF CONDUCTION MATERIAL

We will consider the following single-wire three-phase electrical network (Fig.1):

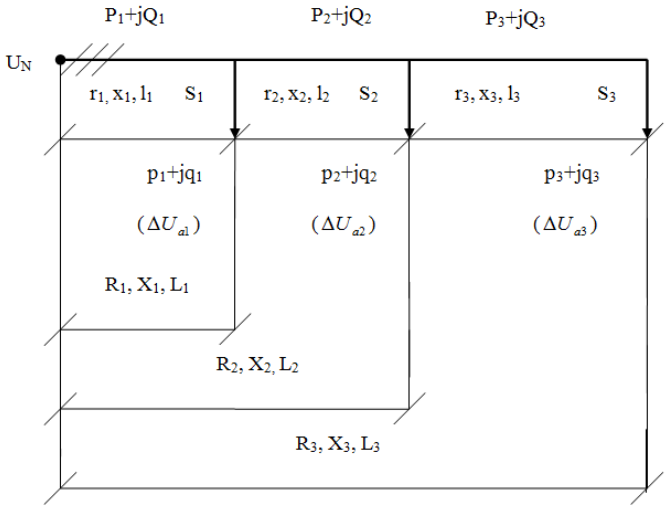

Fig. 1. Three-phase electrical network

where:

U_N – network supply voltage;
r_i, x_i, l_i - resistance, reactance, length of the *i* segment;
R_i, X_i, L_i – resistance, reactance, length of the network part comprised between the supply and the *i* consumer;
P_i+jQ_i – active and reactive powers circulated over the *i* segment;
p_i+jq_i – active and reactive powers circulated on network part comprised between the supply and the *i* consumer;
ΔUai - active voltage loss on the *i* segment;
S_i – section of the *i* segment;
i = 1, 2, 3.

The material volume has to be minimal:

$$V = 3S_1L_1 + 3S_2L_2 + 3S_3L_3 \tag{1}$$

and:

$$\Delta U_a = \Delta U_{a1} + \Delta U_{a2} + \Delta U_{a3} \le \Delta U_{adm} \tag{2}$$

By replacing in V:

$$V = \frac{3\rho P_1 l_1^2}{U_N \Delta U_{a1}} + \frac{3\rho P_2 l_2^2}{U_N \Delta U_{a2}} + \frac{3\rho P_3 l_3^2}{U_N (\Delta U_a - \Delta U_{a1} - \Delta U_{a2})} \tag{3}$$

For optimizing this material function ($V_{\min}$) is applied the derivatives method:

$$\left.\begin{aligned} \frac{\partial V}{\partial (\Delta U_{a1})} = 0 \\ \frac{\partial V}{\partial (\Delta U_{a2})} = 0 \end{aligned}\right\} \tag{4}$$

Solving the system leads to:

$$\frac{S_1}{\sqrt{P_1}} = \frac{S_2}{\sqrt{P_2}} = \frac{S_3}{\sqrt{P_3}} = C_P \tag{5}$$

For „n" segments we will have:

$$S_1 = C_P \sqrt{P_1}\ ;\ S_2 = C_P \sqrt{P_2}\ ;\ S_3 = C_P \sqrt{P_3}\ ;\ \ldots\ldots\ S_n = C_P \sqrt{P_n} \tag{6}$$

In conclusion, the determination of the section in the minimum material volume hypothesis comes down to finding the C_P constant. In order to perform this, there have to be followed several steps [6]:

− a specific average reactance is adopted (x_{0m});

− reactive voltage losses are determined (ΔU_r);

− active voltage losses are determined (ΔU_a).

Specialized literature shows that for the electrical lines made of cables, the calculation error is maintained within admitted limits if there are neglected ΔU_r, ($\Delta U_r \cong 0$) and $\Delta U_a \cong \Delta U_{adm}$.

Because $\rho_1 = \rho_2 = \rho_3 = \ldots\ldots = \rho_n = \rho$ (material being the same; n – number of segments) there may be written:

$$\Delta U_a = \frac{\sum_{i=1}^{i=n} P_i r_i}{U_n} = \frac{\rho}{U_n}\sum_{i=1}^{i=n} P_i \frac{l_i}{S_i} = \frac{\rho}{U_n}\sum_{i=1}^{i=n} \frac{\sqrt{P_i}\sqrt{P_i} l_i}{S_i} = \frac{\rho}{U_n}\sum_{i=1}^{i=n} \frac{\sqrt{P_i} l_i}{\frac{S_i}{\sqrt{P_i}}} = \frac{\rho}{U_n}\sum_{i=1}^{i=n} \frac{\sqrt{P_i} l_i}{C_P} \quad (7)$$

from where:

$$C_P = \frac{\rho \sum_{i=1}^{i=n} \sqrt{P_i} l_i}{U_N \Delta U_a} \quad (8)$$

Therefore, the value of sections can be calculated:

$$S_k = C_P \sqrt{P_k} \quad (9)$$

These sections are normalized, and for standardised sections are taken from the catalogue the values of r_0 and x_0 parameters. Using these values is determined the actual voltage losses on the entire line (ΔU_{real}), which has to fulfil the following condition:

$$\Delta U_{real} = \sqrt{3}\sum_{i=1}^{i=n} (I_{ai} r_i + I_{ri} x_i) \le \Delta U_{adm} \quad (10)$$

If the condition is not fulfilled, there are adopted immediately superior sections and the calculation of ΔU_{real} is performed again.

It is recommended for the sections which result on the network's segments to be verified from the thermal point of view also.

In case of operations performed with loads expressed in currents, the following equations result:

$$\frac{S_1}{\sqrt{I_{a1}}} = \frac{S_2}{\sqrt{I_{a2}}} = \frac{S_3}{\sqrt{I_{a3}}} = ... = \frac{S_n}{\sqrt{I_{an}}} = C_I \quad (11)$$

where I_{an} is the active current on the n segment.

C_I constant is calculated using Equation (12):

$$C_I = \frac{\sqrt{3}\rho}{\Delta U_a}\sum_{i=1}^{i=n} \sqrt{I_{ai}} l_i \quad (12)$$

The sections are given by the following:

$$S_1 = C_I\sqrt{I_{a1}}\ ;\ S_2 = C_I\sqrt{I_{a2}}\ ;\ S_3 = C_I\sqrt{I_{a3}}\ ;\ \ldots\ldots\ S_n = C_I\sqrt{I_{an}} \tag{13}$$

Sections' dimensioning in three-phase networks based on the minimum conduction material consumption are recommended for electrical lines of high length, so that the economy of conduction material to cover the cost of power losses.

For radial arborescent networks (figure 2), analytic formulae for determining optimal sections of power lines are deducted by finding the extremity of the material function (V), using one of the mathematical methods for optimization and the following equations:

$$S_0 = a\frac{M_0}{\Delta U_{a0}}\frac{\sqrt{M_0 I_0} + \sqrt{\sum_{k=1}^{k=n} M_k L_k}}{\sqrt{M_0 L_0}} \tag{14}$$

or indirectly, using the active voltage loss:

$$\Delta U_{a0} = \frac{\Delta U_a}{1 + \dfrac{\sqrt{l_1^2 I_{a1} + \ldots + l_n^2 I_{an}}}{l_0\sqrt{I_{a0}}}} \tag{15}$$

where: $a = \dfrac{\rho}{U_N}$ is a constant which depends on the material and the voltage level;

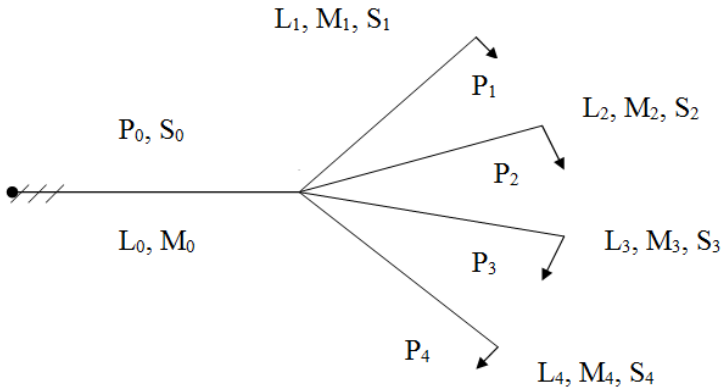

Fig. 2. Radial arborescent network

$M_0 = P_0 L_0\ ;\ M_1 = P_1 L_1\ ;\ \ldots\ldots\ M_n = P_n L_n$ − electrical moment of segments.

Within this method is adopted an additional hypothesis stating that the section of the main column S_0 is equal to the sum of the branches' sections, namely:

$$S_0 = S_1 + S_2 + ... + S_n \tag{16}$$

There results a line with $S = ct.$, but with an equivalent length which is calculated.

3. CONCLUSIONS

The determination of sections of conductors based on the minimum volume of conduction material and of the admitted voltage loss is carried out by establishing the loss of active voltage, admitted for the entire network and afterwards calculating the sections of segments using the known equations.

In the following are adopted the normalized sections which are the closest to the ones resulted from calculation, rounded up or down so that by verifying the total voltage loss to obtain a value as close as possible to the maximum admitted one.

Most high power networks from mining units, but especially the ones from the power system, city power networks or the ones of large companies, which have a significant share in the state's budget, are dimensioned based on this financial criterion.

Regardless the criterion adopted for choosing the section, it has to be verified for all technical-financial conditions from the regulations in force.

REFERENCES

[1]. **Albert, H.,** *Pierderi de putere şi energie în reţelele electrice. Determinare. Măsuri de reducere*, Editura Tehnică, Bucureşti, 1984.

[2]. **Albert, H., Mihăilescu, A.,** *Pierderi de putere şi energie în reţelele electrice*, Editura Tehnică, Bucureşti, 1997.

[3]. **Carabulea, A.,** *Principii şi modele privind proiectarea operaţională a managementului sistemelor de energie*, Editura Academiei Române, Bucureşti, 1996.

[4]. **Conecini, I., şi Dumbravă, V.,** *Bursa de energie electrică*, Editura AGIR, Bucureşti, 2007.

[5]. **Ionescu, D.C.,** *Monitorizarea şi evaluarea continuă a eficienţei energetice*, Editura AGIR, Bucureşti, 2001.

[6]. **Păsculescu, M.F.,** *Instalaţii electrice miniere*, Editura Didactică şi Pedagogică, Bucureşti, 1983.

[7]. **Păsculescu, D., Pădure A.,** *Instalaţii electrice – note de curs*, Editura Universitas, Petroşani, 2010.

[8]. **Răducanu, C.,** *Evaluarea eficienţei energetice. Auditul energetic*, Editura AGIR, Bucureşti, 2007.

[9]. ***** PE 124/93,** *Normativ privind alimentarea cu energie electrică a consumatorilor industriali şi similari*.

VIRTUAL INSTRUMENT USED FOR MONITORING THE SAFETY SWITCHES FROM THE BELT CONVEYORS

NICOLAE PĂTRĂŞCOIU[1] , IOANA CAMELIA BARBU[2], CECILIA ROŞULESCU [3]

Abstract: In this paper we propose a method for monitoring the emergency stop devices for belt conveyors, so that it can be identified which the device has been switched on/off. Depending of the position, on the conveyor route, for the emergency stop device that has been switched on/off is generates a voltage with a custom value. This voltage is transmitted using an appropriate protocol for monitoring and reading the voltage values is possible to identify which of the emergency stop devices has been switched on/off.

Keywords: safety switches, current loop, alarm, belt conveyors, LabVIEW.

1. INTRODUCTION

To stop, in emergency or distress situations, of a conveyor belt for which normal operation or an intervention during operation by an operator requires a robust system to block its operation, so that this lock cannot be raised and it can be canceled only by the direct intervention of an operator.

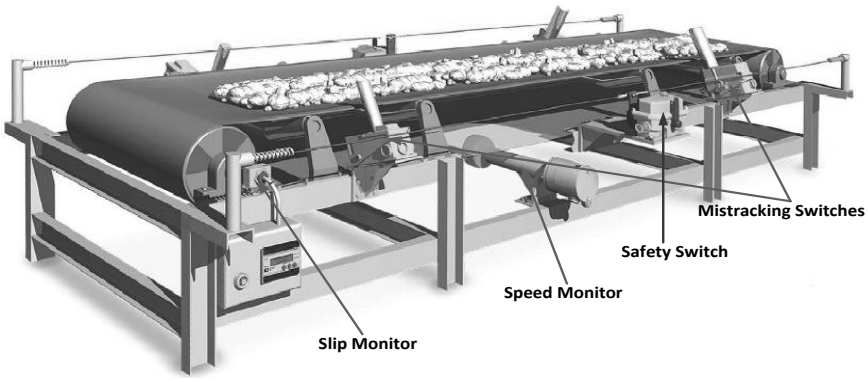

Fig.1. Devices used for monitoring a conveyor belt

[1] *Assoc.Prof., PhD., University of Petrosani*
[2]*Lecturer, PhD., University of Petrosani*
[3]*Professor, Grigore Geamanu School*

These switches called "safety switches" can be operated through a cable stretched across the conveyor to which these devices are mechanically connected, as shown in Fig.1. So by pulling the cable is possible to operate these devices and through them, and so it is possible to emergency stop the operated conveyor.

It is very important to identify the switch actioned so as to be possible to identify the cause that determine its operation and also to make possible an evaluation and elimination of this cause.

The identification can be done locally by means of an optical signal (LED or lamp) which will switch in the "ON" state (or lit) simultaneously with the safety switch actuation. This method has the impediment that requires going through the entire route of the conveyor that may have lengths of tens of meters up to lengths of the order of kilometers.

Much more advantageous, it is the remote monitoring of these safety switches disposed on the conveyor route.

For transmission of information about the safety switches state to the monitoring system can be used the analog transmission of information via the current loop or the digital transmission for witch can be used the RS-485 bus, using different data transmission protocols (Profibus, Modbus) [5].

In Fig. 2 presents a current loop that allows unidirectional transmission of information and it is implemented with two optocouplers, a voltage source and a resistor.

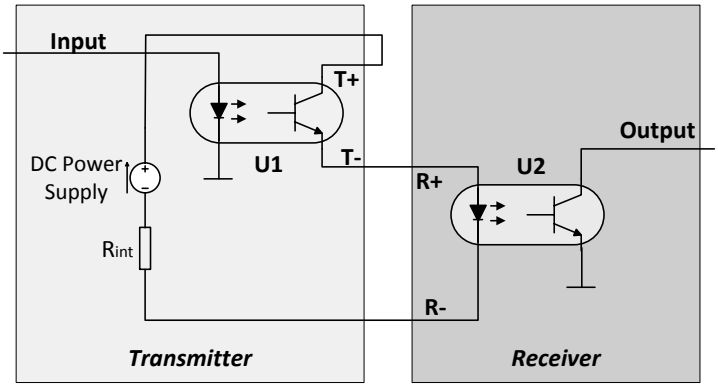

Fig.2. Unidirectional transmission of information via current loop

The optocoupler U1 is emitter and the optocoupler U2, is receiver and the current value, in this circuit, is given by expression:

$$I_{loop} = \frac{(V_S - V_{emitter} - V_{receiver})}{R_S} \tag{1}$$

It can be seen that the current value of the loop current can take different values if VS voltage is variable, also the loop current variations occur and if the resistance value RS has different values [1].

To compensate for this drawback is necessary to use methods and means of maintaining constant current value and RS VS parameter variations.

2. GATHERING INFORMATION ABOUT THE STATE OF SAFETY SWITCHES

To gathering information about the state of the safety switches for every device its contact is coupled with a SPDT type switch with one normally closed contact NC (A) and one normally open contact NO (B).

Through the NO (A) contact, as long as the safety switch is not acted meaning the NO (A) contact is open and the NC (A) contact is closed, a resistor with a specific resistance value is shunted. When the safety switch is operating by opening the contact A and closing the contact B is connected into circuit a LED through which is possible a local identification of the operating device.

In Fig. 3 is shown the wiring diagram of the 10 switches *Si* (*i = 1 ... 10*) which will correspond to 10 devices mounted on the conveyor route.

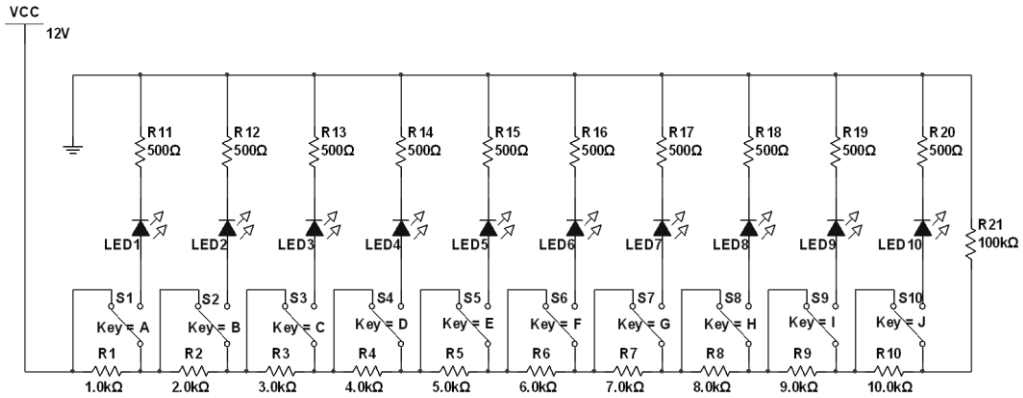

Fig. 3. Wiring the 10 safety switches

Resistors *Ri* (*i = 1 ... 10*) are the resistances that will be shunted accordingly with the operating of the safety switches.

Resistors *Rj* (*j = 11 ... 20*) limits the current to the LEDs indicator *LED 1 ... LED 10*, one for each device.

If is not operate any of the safety switches on the resistance *R21* that form a voltage divider with resistors *R1 ... R10* (shunted in this case) will be a voltage drop of 5 V (equal with supply voltage VCC).

By operating on of the safety switches on the conveyor route is introduced in the circuit resistance *Ri* so that based on the voltage divider relationship will change and the voltage drop across the resistance of the line, meaning that its value will drop from 5V to the extent that index and the resistance will increase, given that the values of these resistors *Ri* are in arithmetic progression

By simulation with Multisim, with some results presented in Fig.4, it can be observe that the size of the output voltage, that is the voltage across the *R21* resistor, is variable relative to the position of the operated safety switch in the conveyor route.

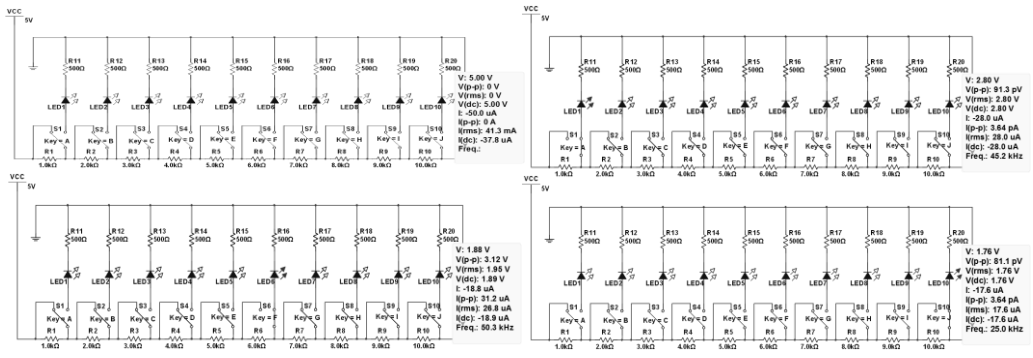

Fig. 4. Circuit simulation

In order to transmit the output value toward the monitoring system is needed to convert obtained voltage to the DC current so as to achieve transmission of information through the unified current 2 – 10 mA or 4 – 20 mA. This conversion is possible to be made by the use of a voltage conversion circuit called voltage-current converter. Such a circuit provides the information transmission lines which may have lengths of hundreds of meters to kilometers order.

The voltage - current converter having the principle diagram shown in Fig.5 is a bidirectional converter with differential input and load connected to ground or other potential without exceeding the dynamic range of the output voltage.

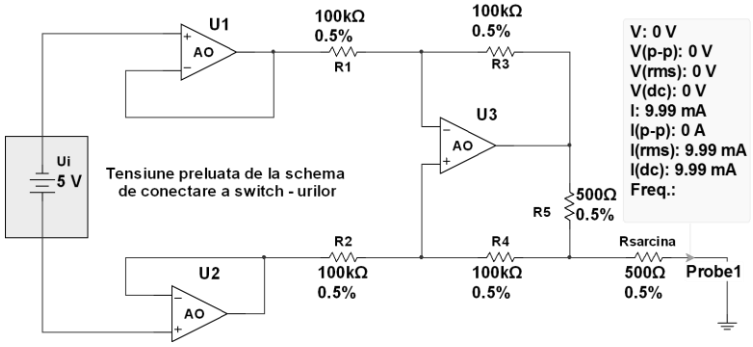

Fig.5. Principle diagram of voltage-current converter

By neglecting the static errors of operational amplifiers, based on condition of the equipotential input ($v^+ = v^-$) for the amplifier U3 and considering VI1 = 0 to simplify the calculation, we obtain the transfer characteristic expression:

$$i_0 = -\frac{v_i}{R_5} \cdot \frac{R_2}{R_1} + \frac{R_2 \cdot R_3 - R_1 \cdot (R_4 + R_5)}{R_1 \cdot (R_3 + R_4)} \cdot \frac{v_o}{R_5} \tag{2}$$

By imposing the following conditions: $R_1 = R_3$ and $R_2 = R_4 + R_5$ the expression of the transfer function becomes:

$$i_0 = -\frac{R_2}{R_1 \cdot R_5} \cdot v_i \tag{3}$$

Since the current loop is used only to transmit information, on the reception is necessary a reverse current-voltage conversion so that it can be possible to use the data acquisition systems for data processing [3].

The most simple current-voltage conversion is to use a calibrated R_C resistor, through which passes the current to be converted, with a resistance value equal to the load resistance of the converter voltage - current. This conversion, suitable from the point of view of the functioning, used for converting the current into voltage, is achieved by means of the operational amplifier, and has the principle diagram shown in Fig.6.

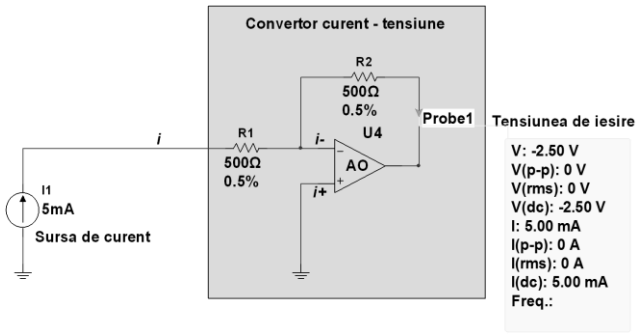

Fig.6. The simulation of the current-voltage converter

The output voltage is proportional to the intensity of the input current and the constant of proportionality (which may serve as scale factor) is the resistance $R=R_1=R_2$.

Exemplification of using of the voltage - current conversion, information transfer via current loop followed by reverse current - voltage conversion, is shown in fig.7.

Here is considered the case of the S10 safety switch operation, so that on output of the switches wiring diagram is obtained the voltage $V=1.76$ which is converted into a current $I_0=3.51$ mA in order to be transmitted through the current loop and on the reception this current is converted into voltage $V_{OUT}=1.76$ V, with the same value as the input.

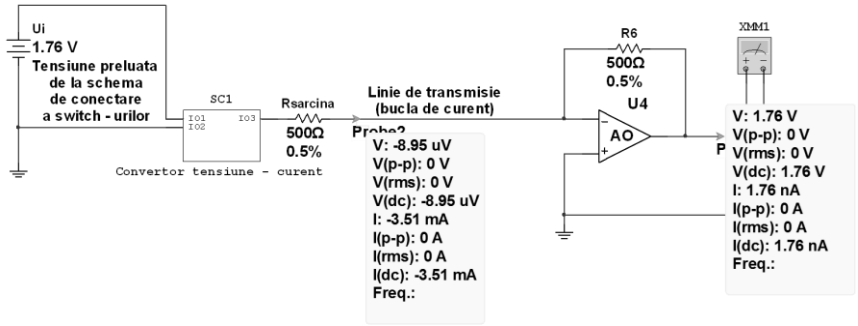

Fig.7. The simulation of current loop transmission

3. VIRTUAL INSTRUMENT USED FOR MONITORING SAFETY SWITCHES

The virtual instrument for monitoring the safety switches disposed on the conveyors route is based on the results obtained by simulating the operation of this monitoring system.

To check the operation of the virtual instrument is made a simulation of this. In this simulation, by operating the one of the safety switches, the proper one of 10 switch configurations is selected.

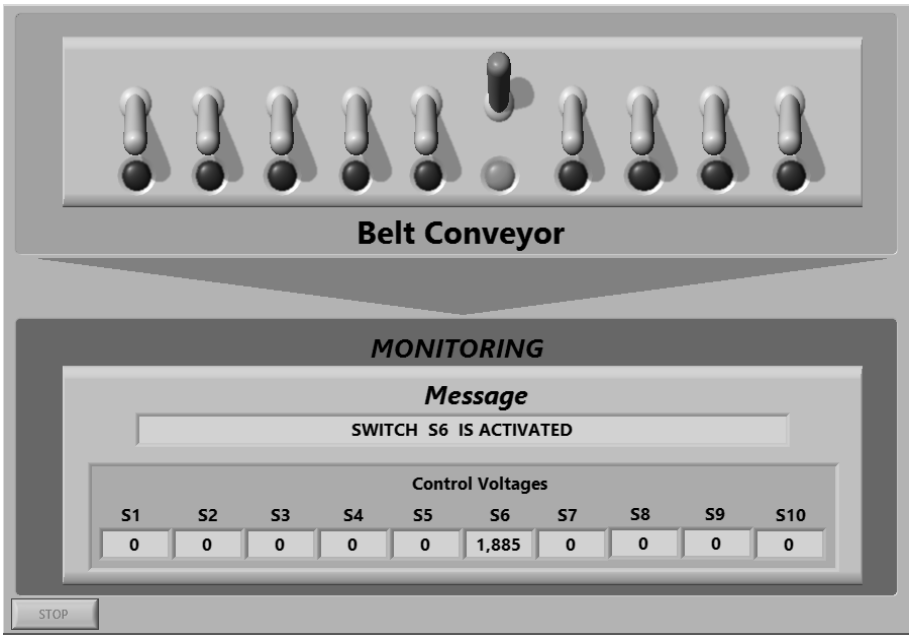

Fig.8. Front panel for operation of switch S6

The front panel of the simulated virtual instrument shown in Fig.8 contains controls represented by the switches *Si* (*i = 1 ... 10*) that simulates the safety switches on the conveyor route. Attached to these controls are LED indicators with role of local signaling device, corresponding to the operated safety switch. Also on the front panel are disposed numerical indicators by which is displayed the voltage obtained by operating each safety switch on conveyor route. If one of the safety switches on the front is acted, by a string indicator is displayed a corresponding message, along with a flash and a sound, to attract the attention of the operator.

Simulation of the system for monitoring the safety switches is obtained by means of the block diagram shown in Fig.9 and that represent the operating program itself.

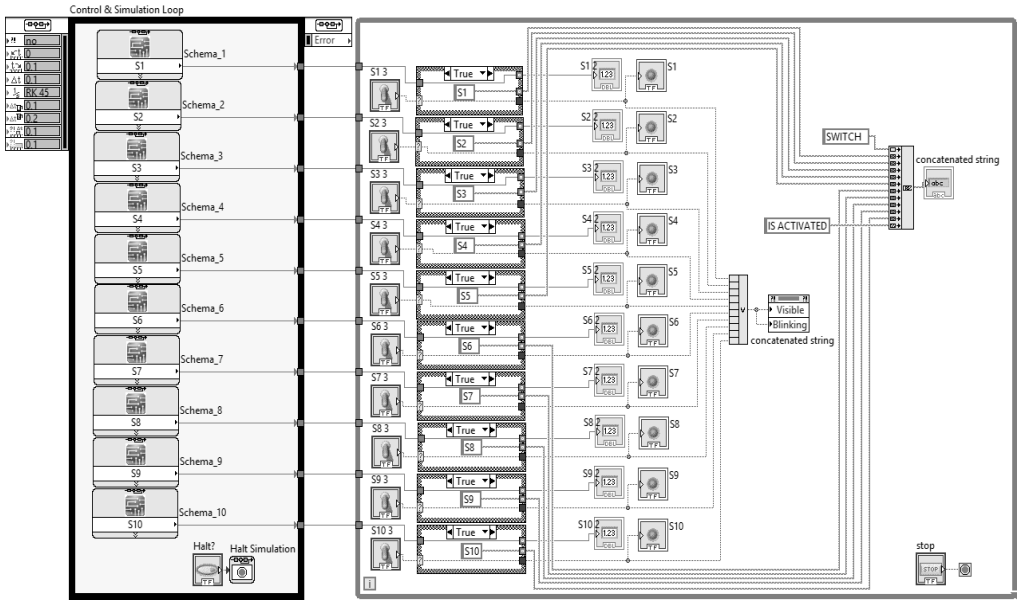

Fig.9. Block diagram of virtual instrument for monitoring system simulation

The program contains two loops, namely:

- Control & Simulation Loop, through which an cyclical reading of switches connection scheme is done to retrieve the appropriate voltage obtained through operation of one switch located along the conveyor;
- While Loop, through which is achieved the voltage signals processing taken from the switches wiring diagram.

Inside the While Loop structure are used Case structures through which is selected the acted switch based on the voltage collected from the Control & Simulation Loop. Once identified the safety switch that is acted a warning is generated and an appropriate message it is displayed by a string indicator. This indicator, without an operation on safety switch, is hidden.

The real functionality of the monitoring system implies the real-time data collected about the status of the safety switches.

As shown above the physical support for data collected from safety switches state is the voltage obtained from resistive divider shown in Fig.3, so that real-time monitoring means reading this voltage. In this case the block diagram representing the real-time monitoring program is shown in Fig.10.

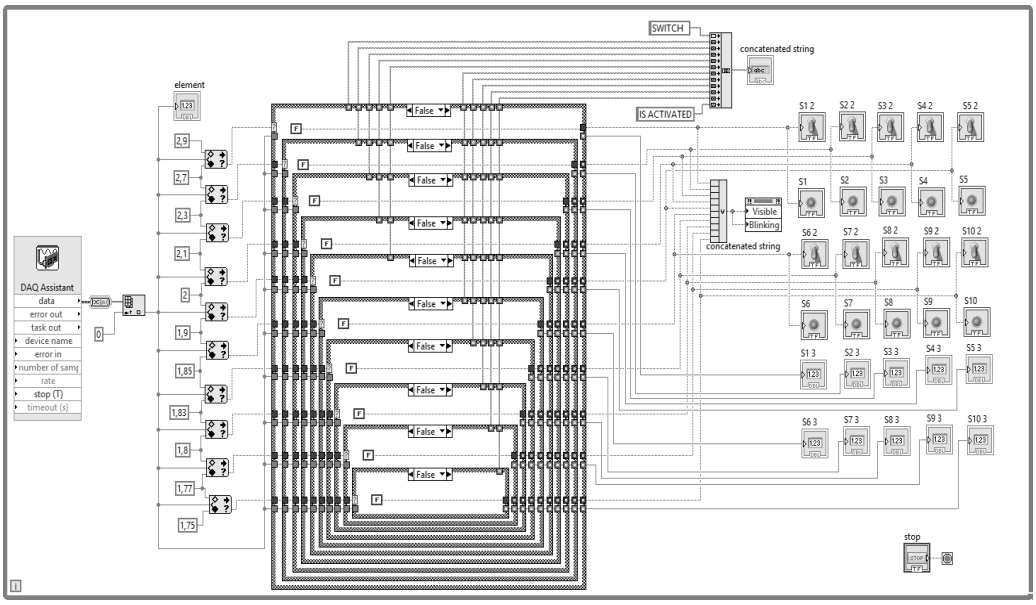

Fig.10. Real-time monitoring program

The voltage collected from the resistive divider, via the DAQ Assistant function, is converted into a string value via the Convert from Dynamic Data Express VI that convert the dynamic data type to numeric data, boolean data, waveform, matrices and other data necessary to be used with other functions or SubVI.

The values of these data are compared with the limits determined by the simulations presented above, using the In Range and Coerce Function that determines whether the x value falls within the specified upper and lower limit of the data.

Framing in the field is made such that the voltage obtained by resistive divider and presented in Table 1 roughly represents the arithmetic mean between the upper and lower limit. In this way the used values are compensated and any deviation of the actual values compared with those calculated and presented in Table 1 is eliminated.

Table 1. Values calculated using resistive divider

Safety switch	***S1***	***S2***	***S3***	***S4***	***S5***	***S6***	***S7***	***S8***	***S9***	***S10***
Voltage [V]	2,798	2,338	2,134	2,017	1,940	1,885	1,843	1,811	1,784	1,762

The range bounded by the two limits that will be determined will activate the LED which corresponds to the operated safety switch. The same interval, through the Case structures, is used to select the number of the safety switch. This number will be added to the string "SWITCH...IS ACTIVATED" resulting in the message "SWITCH ..*i*.. IS ACTIVATED, where *i = 1 ... 10* is the number of the operated safety switch.

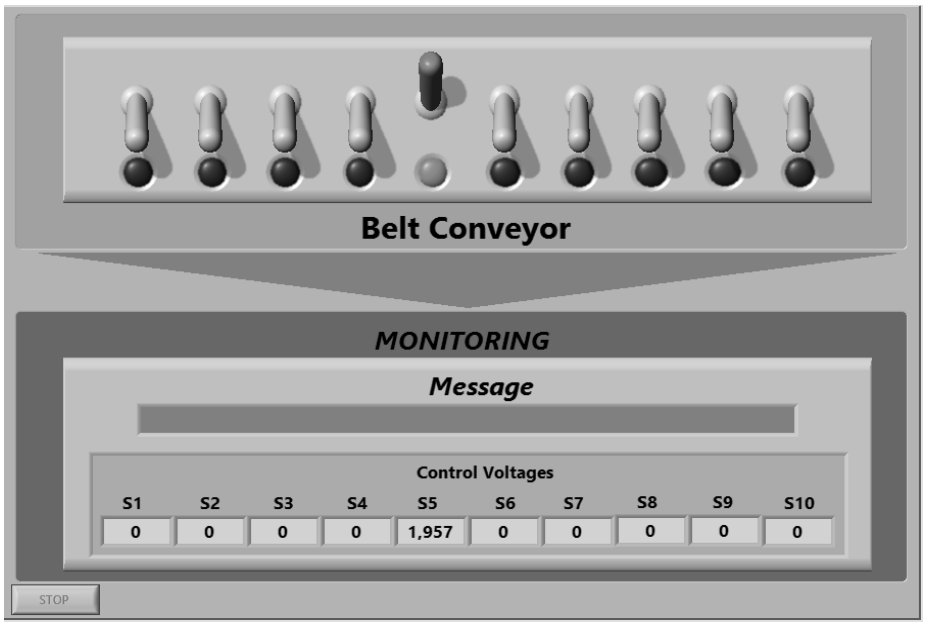

Fig. 11. The front panel of real-time operation

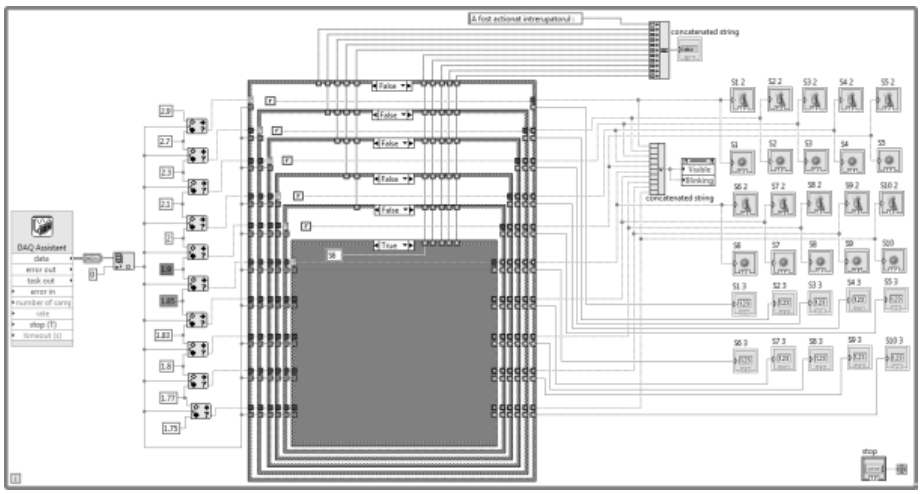

Fig. 12. Real-time monitoring program

In fig.11. is presented the front panel of the virtual instrument which is used for real-time monitoring of the safety switches disposed on route to the belt conveyor and contains the same type of items shown in fig.9.

It sees that the safety switch S6 operation is identified even if the voltage is not exactly 1.885 V but if they fall within the limits [1.90 ... 1.85], as highlighted in the exemplification case through the medium of the block diagram which is shown in Fig.12.

4. CONCLUSIONS

Solution for monitoring the safety switches disposed on conveyor belt route, proposed by this paper has the advantage of simplicity and flexibility. The number of devices is not imposed; it can be set according to the length of the conveyor belt or its configuration. Based on their number can be obtained, through virtual instrument simulation, the voltage values and then the boundaries which include these values.

REFERENCES

[1] **Alan S. M.,** *Measurement and Instrumentation Principles* Butterworth-Heinemann, MA, 2009.

[2] **Bailey D., Wright E.,** *Practical SCADA for Industry*. Elsevier, 2003.

[3] **Beyon J.Y.,** *LabVIEW Programming, Data Acquisition, and Analysis.* Prentice Hall, New York , 2001**.**

[4] **Derenzo E. S.,** *Practical Interfacing in the Laboratory Using a PC for Instrumentation, Data Analysis, and Control* Cambridge University Press, NY, 2003.

[5] **Dunn C. W.,** *Introduction to Instrumentation, Sensors, and Process Control.* Artech House, MA, 2006.

[6] **Sumathi S., Surekha P.**, *LabVIEW based Advanced Instrumentation Systems* Springer-Verlag Berlin Heidelberg, 2007.

[7] *** * *** *Introduction to the Two-Wire Transmitter and the 4-20 mA Current Loop* Whitepaper, http://www.ee.co.za/article/acromag-270-07.html

INDEX OF AUTHORS

REVIEWERS:
Professor, Eng., PhD Susana Arad
Professor, Eng., PhD. Ion Fotău
Scientific researcher II, Eng., PhD. Emilian Ghicioi
Associate Professor, Eng., PhD Nicolae Pătrăşcoiu
Associate Professor, Eng., PhD Marius Marcu
Associate Professor, Eng., PhD Titu Niculescu
Associate Professor, Eng., PhD Ilie Uţu